

## Article

# An Optimization Study on a Novel Mechanical Rubber Tree Tapping Mechanism and Technology

Lingling Wang<sup>1,2</sup>, Chang Huang<sup>1,2</sup>, Tuyu Li<sup>1,2</sup> , Jianhua Cao<sup>1,2</sup>, Yong Zheng<sup>1,2,\*</sup> and Jiajian Huang<sup>3,4,\*</sup>

<sup>1</sup> Rubber Research Institute, Chinese Academy of Tropical Agricultural Sciences, Haikou 571101, China; wanglingling@catas.cn (L.W.); huangchang@catas.cn (C.H.); lituyu@catas.cn (T.L.); cjh1314521@126.com (J.C.)

<sup>2</sup> Mechanical Sub-Center of National Important Tropical Crop Engineering Technology Research Center, Haikou 571101, China

<sup>3</sup> Institute of Scientific and Technical Information, Chinese Academy of Tropical Agricultural Sciences, Haikou 571101, China

<sup>4</sup> Key Laboratory of Applied Research on Tropical Crop Information Technology of Hainan Province, Haikou 571101, China

\* Correspondence: zhengyong07@163.com (Y.Z.); huangjiajian@catas.cn (J.H.);  
Tel.: +86-0898-66961272 (Y.Z.); +86-0898-66862966 (J.H.)

**Abstract:** All-natural rubber is harvested from rubber trees (*Hevea brasiliensis* Muell. Arg.) by traditional tapping knives, so rubber tapping still heavily relies on labor. Therefore, this study explored a novel, hand-held mechanical rubber tapping machine for rubber tree harvesting. In this study, a mechanical tapping cutter with a vertical blade and adjustable guide was first described. The response surface method was applied to evaluate factors affecting the tapping effect. The experimental values were in close agreement with the predicted value. Machine-tapped latex was comparable in quality to hand-tapped latex. Based on the single-factor results, the response surface method (RSM) and the center combined rotation design (CCRD) optimization method were adopted to explore the influence of three factors influencing vertical blade height (A), cutting force (B), and spiral angle (C) on the tapping effect. Regarding the cutting rate of the old rubber line ( $Y_1$ ), cutting time ( $Y_2$ ), latex flow rate ( $Y_3$ ), and average cutting current ( $Y_4$ ) as evaluation indexes of the tapping effect, an optimization scheme was determined. The quadratic model fits for all the responses. The test results showed that the main factors affecting  $Y_1$ ,  $Y_2$ ,  $Y_3$ , and  $Y_4$  were A and B, B, A and C, and B, respectively. Under optimal conditions, the influencing factors of A, B, and C were 10.24 mm, 51.67 N, and  $24.77^\circ$ , respectively, when the evaluation index values of  $Y_1$ ,  $Y_2$ ,  $Y_3$ , and  $Y_4$  were 98%, 8.65 mL/5 min, 9.00 s, and 1.16 A. The range of the relative error between the experimental and predicted results was from  $-11.11\%$  to  $11.11\%$ . According to the optimized treatment scheme, a comparison test was designed between mechanical and manual rubber tapping tools. To verify the availability and effect of the mechanical tapping method preliminarily, the important rubber tapping evaluation indexes included bark thickness, bark excision, latex flow time, cutting time, ash content, and cutting depth, which were selected to serve as a comparison test. There was no significant difference between hand and mechanical methods, except ash content ( $p < 0.05$ ) and cutting time ( $p < 0.01$ ). The mechanical tapping machine proposed in this study is meaningful to improve cutting efficiency, practicality, and operability. Furthermore, it provides crucial theoretical references for the development of intelligent tapping machines.

**Keywords:** *Hevea brasiliensis*; rubber tapping management; old rubber line; hand-held mechanical tapping machine; optimization design; tapping effect



**Citation:** Wang, L.; Huang, C.; Li, T.; Cao, J.; Zheng, Y.; Huang, J. An Optimization Study on a Novel Mechanical Rubber Tree Tapping Mechanism and Technology. *Forests* **2023**, *14*, 2421. <https://doi.org/10.3390/f14122421>

Academic Editor: Eduardo Tolosana

Received: 2 November 2023

Revised: 1 December 2023

Accepted: 10 December 2023

Published: 12 December 2023



**Copyright:** © 2023 by the authors. Licensee MDPI, Basel, Switzerland. This article is an open access article distributed under the terms and conditions of the Creative Commons Attribution (CC BY) license (<https://creativecommons.org/licenses/by/4.0/>).

## 1. Introduction

Rubber trees (*Hevea brasiliensis* Muell. Arg.) are significant industrial crops that are primarily cultivated in tropical and semi-tropical countries, such as India, Indonesia, Malaysia, Thailand, Vietnam, and Hainan, Yunnan, and Guangdong provinces of China [1,2]. As

latex is harvested from rubber trees, natural rubber serves as an essential industrial raw material and strategic material [3]. It is widely used in the fields of aerospace, national defense, transportation, medicine, hygiene, and daily life [4]. Its unique tensile crystallization properties make it irreplaceable, particularly in aircraft tires operating under complex load conditions [5,6].

Natural rubber is extracted from the lactiferous vessels of rubber trees via regular tapping [7,8], making rubber tapping the only method of obtaining it [9–11]. Consequently, rubber tapping has become a vital occupation for rubber farmers [12], so the tapping work relies heavily on labor [13]. As perennial crops, rubber trees are usually cultivated assuming a lifespan of 30 years based on the technical feasibility of the management of tapping panels [14]. Large-scale planting of rubber trees has been ongoing for over 100 years, and traditional rubber panel cutting techniques still rely on traditional manpower knives to cut rubber bark. It is considered to be a skill-oriented job, and unskilled laborers should not use the traditional V-groove knife or Jabong knife because it is very difficult for a novice worker to control the depth, thickness, and slope of the tapping angle. A tapping task is usually made of 500 to 700 trees and is completed in 3–4 h. Tapping workers need to get up at 2:00 am and begin work in rubber plantations using traditional tapping knives without power. Rubber tapping is labor intensive, time consuming, not efficient, and has high labor costs [15]. The decline in skilled workers, low incomes, and increased labor charges have become increasingly significant issues in rubber production [16–19]. Therefore, tapping skills and machinery are key factors influencing the low efficiency of manual tapping.

As shown in Figure 1, the complex contour curve of the rubber tree trunk is hard to fit using a tapping machine [20]. The growth of rubber tree trunks is uneven, and the thickness of the bark is also irregular even within the same trunk [21]. Traditional tapping tools require a manual to control the cutting trajectory, making the process challenging and inefficient. During rubber tapping, a uniform tapping depth and a straight, smooth tapping line are necessary, resulting in high design requirements for rubber tapping machinery. The bark comprises a water capsule skin, yellow skin, an inner layer of sand skin, an outer layer of sand skin, and coarse skin from the inside to the outside. Yellow bark contains many highly functional mature latex tube laticifers and is the main rubber-producing part [22]. The water capsule skin includes a functional secondary phloem and cambium, with a thickness usually less than 1 mm. Damage to the water capsule skin will diminish latex yield.

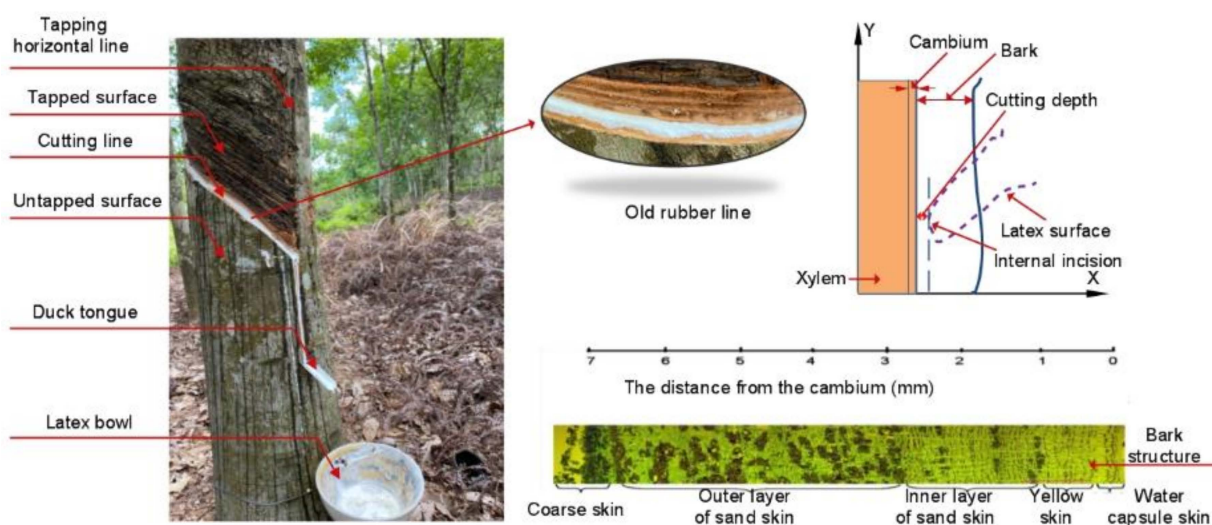


**Figure 1.** Tapping surface and anatomical bark structure of a rubber tree.

Harvested as latex from rubber trees, natural rubber is an aqueous emulsion that is prone to adhesion, efflux, and contamination. The old rubber line (shown in Figure 1)

left after rubber tapping exhibits high elasticity, making it necessary to manually remove it before tapping. The bark stripped should not contaminate the harvesting latex. It is essential to avoid entangling the old rubber line with knives as much as possible, and the bark stripping must not generate debris. In natural rubber production, the number of lactiferous vessels in the bark is closely related to latex yield [22]. The cells of lactiferous vessels in rubber trees exhibited high phloem turgor pressure, which varies from 8 to 12 bar due to water withdrawal from transpiration [23–25]. The mechanical tissue of the bark serves a supportive and protective role, ensuring the tree's standing and resistance to external forces. Rubber bark is hard and difficult to cut. As rubber trees are perennial crops, it is crucial to avoid harming the cambium during tapping, and the cutting depth (shown in Figure 1) should be between 1.2 mm and 1.8 mm. Rubber tapping evaluation indexes, bark thickness, bark excision, latex flow time, cutting time, ash content, and cutting depth are important for rubber production.

Rubber plantations are mostly distributed in hilly and mountainous areas with significant terrain differences, impeding the development of agricultural mechanization [26,27]. Over the past decade, research on rubber tapping machines and technologies has developed rapidly. Rubber tapping machines include electrical tapping knives, fixed tapping machines, and self-propelled rubber tapping robots [13,19,22] (shown in Figure 2). This approach could effectively reduce the technical difficulty and labor intensity in tapping panel cutting. However, most of the equipment is still in the laboratory stage and has not yet reached the stage of industrialization and commercial use [13,22]. In the research on mechanical tapping machine design, mechanical parameters, tapping agronomy, and tapping effects are the current focus [13,19,22]. The mechanical parameters mainly include the cutting blade, guide, weight, gear, and power. Tapping agronomy mainly includes cutting force, spiral angle, cutting line, and cutting current. The tapping effect mainly includes bark thickness, bark excision, latex flow time, cutting time, ash content, and the cutting rate of old rubber lines. The cutting time for a single rubber tree tapping is adopted to evaluate mechanical tapping efficiency generally [13,19,22].

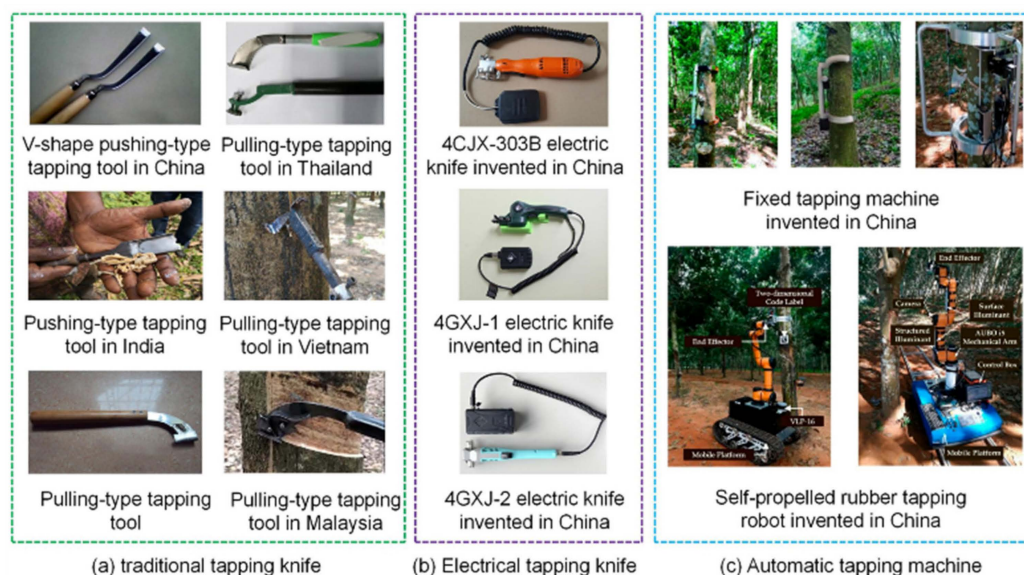


**Figure 2.** Examples of rubber tapping equipment and technology.

Response surface methods are rarely applied in agricultural research in recent years [28,29] and are mainly applied in industrial, energy, chemistry, and biology [30–38]. New theories commonly used in mechanical optimization design include meta-heuristic approaches, the chaotic levy flight distribution algorithm, artificial intelligence algorithms, the level set method, the ant lion optimizer, and the sine cosine algorithm [39–44].

A V-shaped blade, a circular saw blade, and a blade with only a horizontal edge are commonly applied in mechanical rubber tapping machines [13,19,22,45,46]. A mechanical

rubber tapping mechanism with a vertical blade and adjustable guide is first proposed (shown in Appendix A). The vertical blade height is first considered as a key factor influencing the cutting rate of old rubber lines. Therefore, we hypothesized that mechanical tapping machines could strip old rubber lines from rubber trees easily, reduce physical demands, decrease reliance on skilled workers, and improve cutting efficiency and operability on rubber tapping. The study of a novel, hand-held mechanical rubber tapping machine was, therefore, conducted to (1) analyze the mechanical rubber tapping mechanism with a vertical blade and adjustable guide; (2) determine significant influencing factors; (3) determine an optimization scheme and establish quadratic models; and (4) determine an efficient and operational hand-held mechanical tapping method.

## 2. Materials and Methods

### 2.1. Experimental Site Characteristics

Rubber cutting experiments using a mechanical rubber tapping machine were conducted at the experimental farm of the Chinese Academy of Tropical Agricultural Sciences, Danzhou City, Hainan Province, China (19°58'18" N, 109°49'51" E, altitude 110 m). The experiment site's climate was classified as a tropical monsoon climate, with an annual average temperature of approximately 23.5 °C, annual average sunshine of about 2500 h, annual average rainfall of around 1815 mm, and a frost-free period of over 280 days. Rubber tapping was conducted annually from April to December. The annual solar radiation energy received ranges from 110 to 130 kilocalories per square centimeter. The average annual rainfall was 1815 mm.

### 2.2. Field Experiment Design

Firstly, taking the influencing factors A and B as variable influence factors, a single-factor test was designed to determine the factor parameters and narrow the optimization level range of each factor for the response surface analysis. Secondly, based on the single-factor results, the response surface method (RSM) and the center combined rotation design (CCRD) optimization method were adopted to explore the influence of three influencing factors involved, A, B, and C, on the tapping effect of  $Y_1$ ,  $Y_2$ ,  $Y_3$ , and  $Y_4$ . Thirdly, according to the optimized treatment scheme, a comparison test was designed between mechanical and manual rubber tapping tools to determine and verify the availability and effect of the mechanical tapping method.

Single-factor test. Take 20 rows  $\times$  40 lines of rubber forest as the test subject, removing the trees of newly replanted, sick, rubber trunk perimeters of less than 600 mm and remove the old rubber line. Then, 20 sample trees were selected by a machine to carry out the single-factor test of rubber tapping. According to the result of blade parameters and force analysis in Appendix B, the main factors of the blade friction forces were cutting force, vertical blade height, spiral angle, and angle of the blade edge. In the common traditional method of hand rubber tapping, the range of the spiral angle was 20–30°, and the angle of the blade edge was 4°. All these reliability data could give reference in mechanical tapping tests. In order to determine the range of cutting force and vertical blade height, a single-factor experimental design was used (shown in Table 1).

**Table 1.** Single-factor experimental design.

Variable Factor	Variable Level	Test Condition
Vertical blade height (A) $L_2$ /mm	6, 8, 10, 12, 14	Trunk diameter of more than 600 mm with the old rubber line and healthy trees.
Cutting force (B) F/N	30, 40, 50, 60, 70	

Response surface optimization test. In the common traditional method of hand rubber tapping, the spiral angle was in the range of 20–30°, and the angle of the blade edge was 4°. The range of vertical blade height and cutting force could be determined by a single-factor test. Therefore, three influence factors, vertical blade height, cutting force, and spiral angle,

were adopted in the response surface optimization test. The center combined rotation design (CCRD) optimization method involved three influence factors, A, B, and C, and was designed to explore the interaction of three influencing factors on the tapping effect of  $Y_1$ ,  $Y_2$ ,  $Y_3$ , and  $Y_4$ . According to the level range of each factor determined in the single-factor test, the center combination rotation design method was adopted to determine the analytical factors and levels. Analytical factors and levels based on response surface methodology were designed (shown in Table 2). According to response surface methodology and the structure matrix designed by three orthogonal rotations, three influence factors needed 20 standard tests [28,29] (shown in Table 3). Take 20 rows  $\times$  40 lines of rubber forest as the test subject, removing the trees of newly replanted, sick, rubber trunk perimeters of less than 600 mm and remove the old rubber line. Then, 20 sample trees were selected by a machine to carry out the response surface optimization test of the rubber tapping.

**Table 2.** Analytical factors and levels based on response surface methodology.

Level Code	Variable Level		Test Condition	
	Vertical Blade Height (A)	Cutting Force (B)	Spiral Angle (C)	
	L <sub>2</sub> /mm		F/N	$\theta/^\circ$
−1	8.00	40.00	20.00	
0	10.00	50.00	25.00	
1	12.00	60.00	30.00	

**Table 3.** Experimental design and results.

Test Number	Level Code			Cutting Rate of Old Rubber Line (Y1)/%	Cutting Time (Y2)/s	Latex Flow Rate (Y3)/mL/5 min	Average Cutting Current (Y4)/A
	A (Vertical Blade Height)	B (Cutting Force)	C (Spiral Angle)				
1	−1	−1	−1	35	23	2.1	1.22
2	1	−1	−1	100	25	7.3	0.98
3	−1	1	−1	76	10	7.3	1.28
4	1	1	−1	100	9	9.4	1.23
5	−1	−1	1	64	23	4.1	1.21
6	1	−1	1	100	26	11.1	1
7	−1	1	1	75	8	7	1.11
8	1	1	1	100	12	9.2	1.35
9	−1.682	0	0	27	14	2.5	1.34
10	1.682	0	0	100	12	10.8	1.19
11	0	−1.682	0	92	32	8.8	0.86
12	0	1.682	0	94	8	9.1	1.29
13	0	0	−1.682	100	11	6.2	1.23
14	0	0	1.682	98	15	9.8	1.54
15	0	0	0	95	13	8.2	1.28
16	0	0	0	100	16	7.8	1.02
17	0	0	0	96	12	8.9	0.99
18	0	0	0	85	10	8.6	1.19
19	0	0	0	95	15	9.1	1.11
20	0	0	0	100	13	7.3	1.28

**Comparison test:** To verify the availability and effect of the mechanical tapping method, a comparison test between two tapping tools of a V-shape pushing type tapping tool and a hand-held mechanical rubber tapping machine using the mechanical cutter was designed using the optimized treatment scheme. Take 20 rows  $\times$  40 lines of rubber forest as the test subject, removing the trees of newly replanted, sick, rubber trunk perimeters of less than 600 mm and remove the old rubber line. Then, the same 30 sample trees tapped using mechanical and hand tapping methods were selected to carry out the comparison test (shown in Table 4) and cutting current test. Rubber trees were tapped once per three days

in the test. Bark thickness, bark excision, latex flow time, cutting time, ash content, and cutting depth were selected as rubber tapping evaluation indexes. The evaluation indexes were used in rubber production.

**Table 4.** A comparison test design of rubber tapping using two methods alternately.

Rubber Tapping Sequence	Tapping Method	Results	Rubber Tapping Evaluation Indexes
1	Mechanical	Mechanical 1	Bark thickness, bark excision, latex flow time, cutting time, ash content, and cutting depth
2	Hand	Hand 1	
3	Mechanical	Mechanical 2	
4	Hand	Hand 2	
5	Mechanical	Mechanical 3	
6	hand	Hand 3	

Mechanical result = (Mechanical 1 + Mechanical 2 + Mechanical 3)/3. Hand result = (Hand 1 + Hand 2 + Hand 3)/3.

According to the traditional rubber tapping method, a cutting depth of 1.2–1.8 mm was employed. When using the mechanical tapping machine (shown in Appendix A), it was necessary to turn on the power for 5 s to ensure that the machine entered a stable operating state. A tape measure, Vernier caliper, calculagraph, weighing meter, and an RH2010SF-1 latex dry content tester were used to acquire the experimental data. A Vernier caliper was used to measure bark thickness and excised bark, a stopwatch was used to measure cutting time and latex flow time, an RH2010SF-1 latex dry content tester was used to assess dry rubber content, and a weighing meter was used to weigh the latex. This allowed for the observation of bark thickness and bark excision, latex flow time, cutting time, ash content, cutting depth, and cutting current.

### 2.3. Field Measurements

The cutting rate of the old rubber line can be calculated based on the length of the old rubber line before and after tapping. The cutting rate of the old rubber line = (length of the old adhesive line cut out/total length of the old adhesive line) × 100%.

Cutting time: The time required to complete a single rubber tree tapping in seconds.

Latex flow rate: Yield of latex within 5 min for a single rubber tree tapping. It is described in mL/5 min.

Bark thickness: The thickness of the bark is excised by the cutter. It is described in millimeters.

Bark excision width. The width of the bark is excised by the cutter. It is described in millimeters.

Cutting depth is calculated based on the total thickness of the bark and the thickness of the bark excised in millimeters. Cutting depth = total thickness of bark—the thickness of bark cut off.

Ash content: The rubber latex that flowed out after tapping is incinerated at low temperatures and then incinerated at 520–550 °C. The organic matter is burned, and the remaining part is the oxide of metal elements, which is the ash content of the rubber latex. It is placed in a desiccant until it reaches a balanced weight, and it is measured by weight. The ash content of rubber latex is calculated as (latex ash weight/latex weight) × 100%.

No-load current: Stable current after starting the machine power before rubber tapping. The no-load current is measured in amperes (A).

Maximum cutting current is the maximum current during rubber tapping. It is described in amperes (A).

Minimum cutting current is the minimum current during rubber tapping. It is described in amperes (A).

## 2.4. Data Analysis and Processing

Data were processed using Microsoft Excel 2010, Design-Expert 12, and Origin 20.8, and SPSS 27.0. Design-Expert 12 was used for data statistics and response surface analysis. SPSS (version 27.0) was used for sample significance analysis, and an independent sample *t*-test was used for significance analysis. A flowchart of the study is shown in Figure 3.

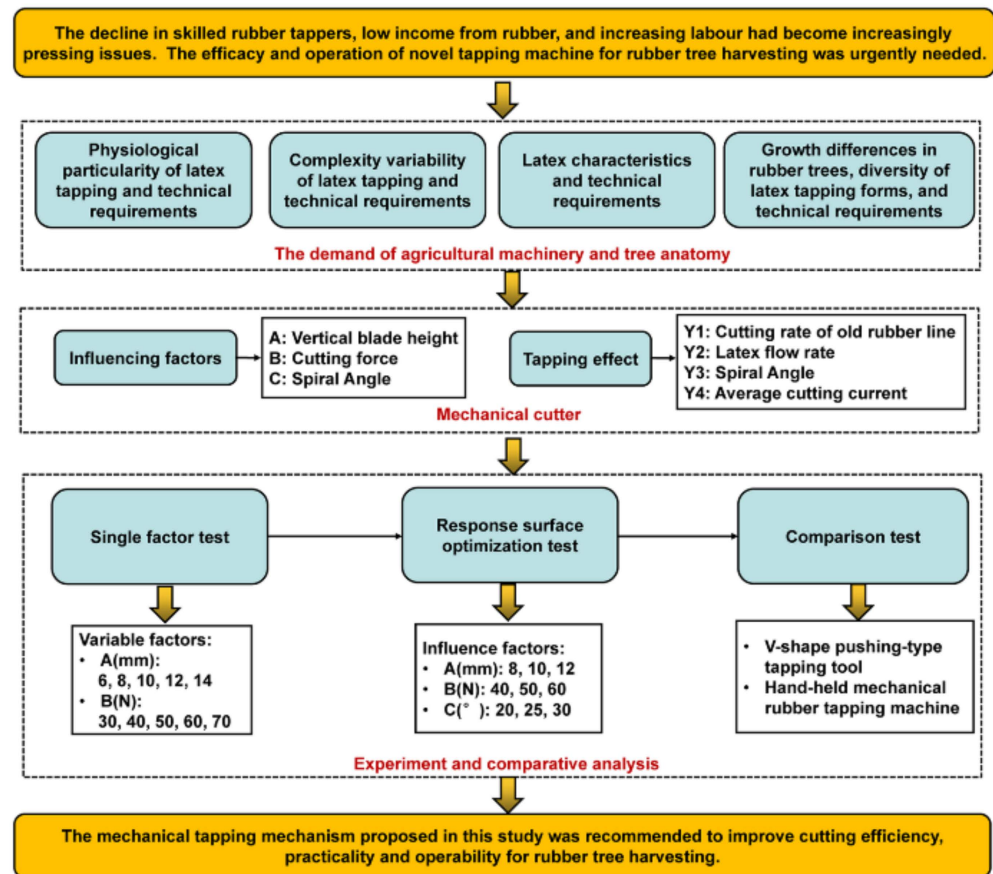


Figure 3. Flowchart of the research.

## 3. Results

The mechanical cutter applied in rubber tree harvesting, good tapping quality, and stability were considered. Therefore, the test focused on the tapping quality and stability of the mechanical cutter. Single-factor experimental test results determined the range of cutting force and vertical blade height. Variance analysis of the regression model for the response surface established the fitted second-order polynomial equation between three influencing factors and tapping effects. Interaction results for response surface described the various response surface 3D graphs for the interaction of the three factors on the tapping effect. The comparison test verified the availability and effect of the mechanical tapping method preliminarily.

### 3.1. Single-Factor Test Results

As the vertical blade height increased, the cutting rate of the old rubber line and latex flow rate both increased rapidly; the cutting time reduced rapidly, but the average cutting current was not significant (shown in Figure 4). According to the results of the single-factor test, when the evaluation index results of  $Y_1$ ,  $Y_2$ ,  $Y_3$ , and  $Y_4$  were approximately 95%, 8.50 mL/5 min, 13.00 s, and 1.20 A, respectively, the influencing factor of the vertical blade height was 10 mm. Due to differences in the old rubber lines, the cutting rates of the old rubber lines with blades of different heights might change in a range of variations (shown in Figure 4a). Thin old rubber lines were easier to cut, whereas thick old rubber

lines were more difficult to cut. The variation range of the cutting rate, using blades with heights of 6, 8, 10, 12, and 14 mm, was 20%, 20%, 5%, and 0, respectively. When the blade height exceeded 10 mm, the cutting rate of the old rubber line remained relatively stable. It indicated that the blade had a critical value for stripping the old rubber line.

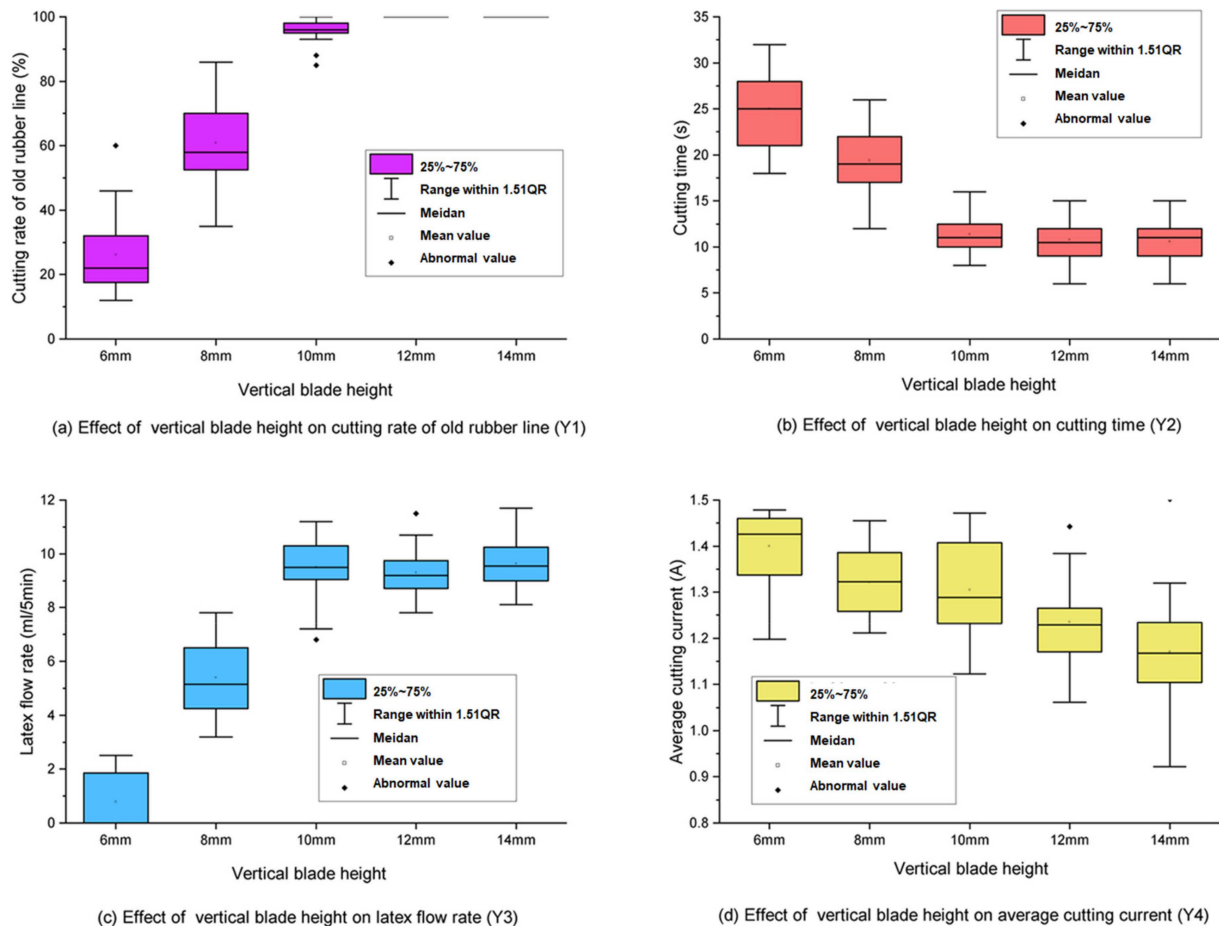


**Figure 4.** The effects of the vertical blade height (A) on the tapping effect of  $Y_1$ ,  $Y_2$ ,  $Y_3$ , and  $Y_4$ .  $Y_1$ ,  $Y_2$ ,  $Y_3$ , and  $Y_4$  were the cutting rate of the old rubber line, cutting time, latex flow rate, and average cutting current, respectively.

The average cutting rates of the old rubber lines, using blades with heights of 6, 8, 10, 12, and 14 mm, were 25%, 60%, 95%, 100%, and 100%, respectively. The shorter blades with cutting rates of 60 and 25% allowed old rubber lines to wrap around the knife and interfere with the cutting trajectory. The taller blades with cutting rates of 95 and 100% easily striped the old rubber lines from the tapping panel. Before rubber tapping, there was no need to manually tear the old rubber lines using a blade with a height of more than 10 mm. The results and effects of using cutting blades with varying heights to cut old rubber lines are shown in Figure 5.

As the cutting force increased, the cutting rate of the old rubber line and latex flow rate both increased rapidly, and the cutting time and average cutting current reduced rapidly (shown in Figure 6). As the cutting force increased from 30 N to 50 N, the variation ranges of  $Y_1$ ,  $Y_2$ ,  $Y_3$ , and  $Y_4$  reduced significantly and tended to be stable. As the cutting force increased from 50 N to 70 N, the variation ranges of  $Y_1$ ,  $Y_2$ ,  $Y_3$ , and  $Y_4$  were not significant. According to the results of the single-factor test, when the evaluation index results of  $Y_1$ ,  $Y_2$ ,  $Y_3$ , and  $Y_4$  were approximately 95%, 8.50 mL/5 min, 13.00 s, and 1.20 A, respectively, the influencing factor of the cutting force was 50 N.

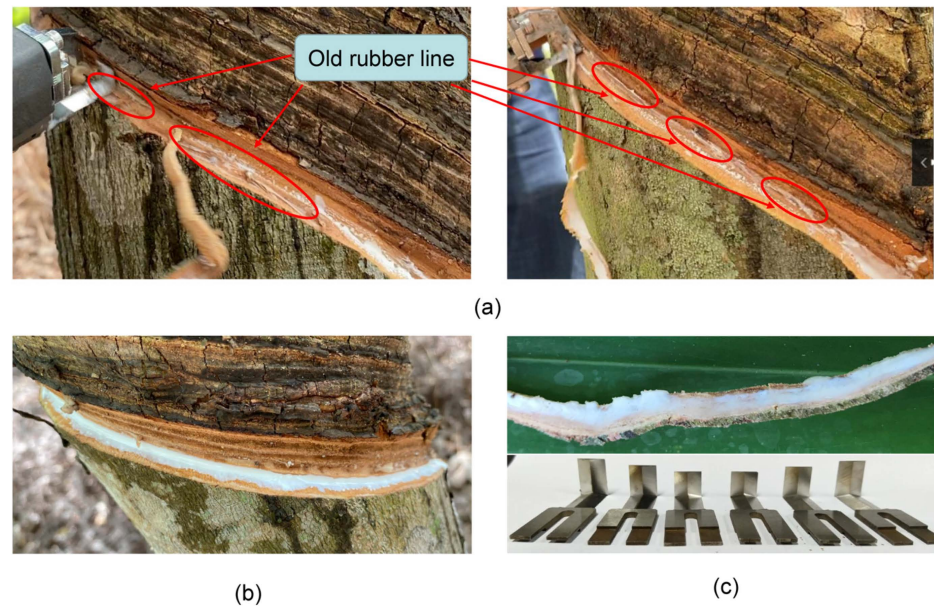


**Figure 5.** Results and effects of using cutting blades with varying heights to cut old rubber lines: (a) the cutting rate of the old rubber line below 100%, (b) a 100% cutting rate of the old rubber line, (c) a complete old rubber line and different height blades. Blade heights from left to right were 14 mm, 10 mm, 8 mm, 6 mm, 12 mm, and 14 mm, respectively.

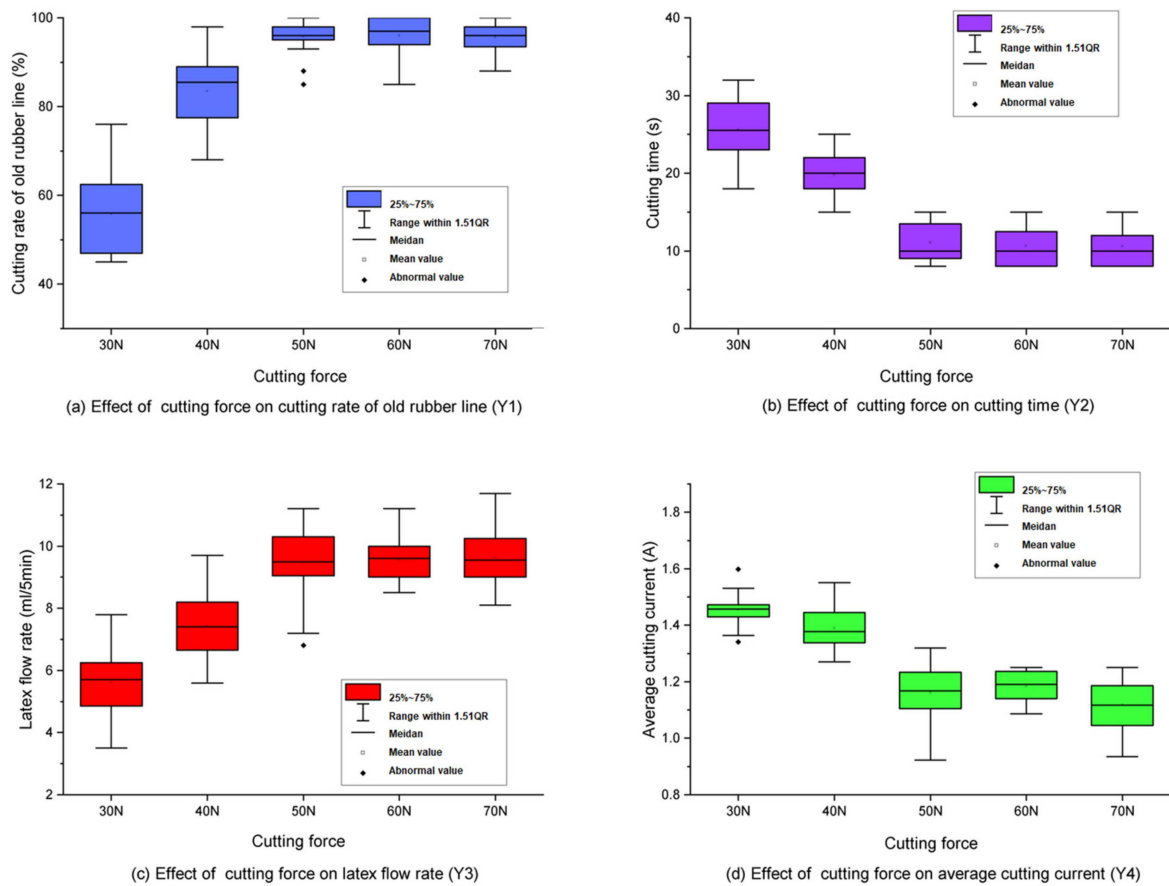


**Figure 6.** The effects of the cutting force (B) on the tapping effect of  $Y_1$ ,  $Y_2$ ,  $Y_3$ , and  $Y_4$ .  $Y_1$ ,  $Y_2$ ,  $Y_3$ , and  $Y_4$  were the cutting rate of the old rubber line, cutting time, latex flow rate, and average cutting current, respectively.

### 3.2. Variance Analysis of the Regression Model for Response Surface

According to the single-factor test results, Design-Expert 12 software was used to conduct statistical and response surface analysis to determine the optimal scheme of the mechanical cutter. The experimental design and results are shown in Table 3.

According to the experimental results in Table 4, multiple regression fitting analysis was used to establish the fitted second-order polynomial equation between the three influencing factors and tapping effects of  $Y_1$ ,  $Y_2$ ,  $Y_3$ , and  $Y_4$ . The fitted second-order polynomial equations showed:

$$\begin{cases} Y_1 = -695.18 + 94.46A + 6.99B + 6.30C - 0.33AB - 0.35AC - 0.08BC - 2.97A^2 - 0.01B^2 + 0.03C^2 \\ Y_2 = 138.49 - 2.41A - 3.34B - 1.15C - 0.01AB - 0.08AC + 0.07A^2 + 0.03B^2 + 0.01C^2 \\ Y_3 = -70.88 + 6.62A + 0.87B + 1.22C - 0.05AB + 0.02AC - 0.02BC - 0.18A^2 - 0.01C^2 \\ Y_4 = 4.88 - 0.45A + 0.01B - 0.16C + 0.01A^2 \end{cases} \quad (1)$$

The fitted second-order polynomial equation after the non-significant factors were removed showed:

$$\begin{cases} Y_1 = -695.18 + 94.46A - 0.33AB - 2.97A^2 \\ Y_2 = 138.49 - 3.34B + 0.03B^2 \\ Y_3 = -70.88 + 6.62A + 0.87B + 1.22C - 0.05AB - 0.02BC - 0.18A^2 \\ Y_4 = 4.88 + 0.01B \end{cases} \quad (2)$$

Variance analysis of the regression model for response surface on the cutting rate of the old rubber line ( $Y_1$ ), cutting time ( $Y_2$ ), latex flow rate ( $Y_3$ ), and average cutting current ( $Y_4$ ) is shown in Table 5, Table 6, Table 7, and Table 8, respectively. The non-significant value of the lack of fit ( $p = 0.19$ ,  $p > 0.05$ ) showed that the model was fitted with good prediction ( $R^2 = 0.94$ ) (shown in Table 5). Various factors showed a significant effect on the cutting rate of old rubber lines. These were linear (A), interactive (AB), and quadratic ( $A^2$ ) effects. The vertical blade height (A) produced a maximum effect on the cutting rate of old rubber lines. Based on the F test result, the impact order showed vertical blade height (A) > cutting force (B) > spiral angle (C).

**Table 5.** Variance analysis of the regression model for response surface on the cutting rate of old rubber lines.

Source	Sum of Squares	df	Mean Square	F-Value	p-Value	Level of Significance
Model	8356.46	9	928.5	18.63	<0.0001	***
A (vertical blade height)	5448.1	1	5448.1	109.32	<0.0001	***
B (cutting force)	224.44	1	224.44	4.5	0.0598	-
C (spiral angle)	44.44	1	44.44	0.8918	0.3672	-
AB	338	1	338	6.78	0.0263	*
AC	98	1	98	1.97	0.1911	-
BC	112.5	1	112.5	2.26	0.1639	-
$A^2$	2038.85	1	2038.85	40.91	<0.0001	***
$B^2$	30.91	1	30.91	0.6203	0.4492	-
$C^2$	6.22	1	6.22	0.1247	0.7313	-
Residual	498.34	10	49.83			
Lack of fit	347.51	5	69.5	2.3	0.1905	-
Pure error	150.83	5	30.17			
Cor Total	8854.8	19				

$R^2 = 0.94$ ;  $R^2_{adj} = 0.89$ ;  $R^2_{pre} = 0.66$

$R^2$  = coefficient of determination,  $R^2_{adj}$  = adjusted  $R^2$ ,  $R^2_{pre}$  = predicted  $R^2$ . Level of significance \*\*\*  $p < 0.001$ , \*  $p < 0.05$ .

**Table 6.** Variance analysis of the regression model for the response surface on cutting time.

Source	Sum of Squares	df	Mean Square	F-Value	p-Value	Level of Significance
Model	828.8	9	92.09	21.05	<0.0001	***
A (vertical blade height)	1.57	1	1.57	0.3598	0.562	-
B (cutting force)	708.46	1	708.46	161.92	<0.0001	***
C (spiral angle)	5.58	1	5.58	1.27	0.2853	-
AB	0.5	1	0.5	0.1143	0.7423	-
AC	4.5	1	4.5	1.03	0.3344	-
BC	0	1	0	0	1	-
A <sup>2</sup>	1.01	1	1.01	0.2314	0.6409	-
B <sup>2</sup>	108.19	1	108.19	24.73	0.0006	***
C <sup>2</sup>	1.01	1	1.01	0.2314	0.6409	-
Residual	43.75	10	4.38			
Lack of fit	20.92	5	4.18	0.9162	0.5371	-
Pure error	22.83	5	4.57			
Cor total	872.55	19				

 $R^2 = 0.95; R^2_{adj} = 0.90; R^2_{pre} = 0.78$ 
 $R^2$  = coefficient of determination,  $R^2_{adj}$  = adjusted  $R^2$ ,  $R^2_{pre}$  = predicted  $R^2$ . Level of significance \*\*\*  $p < 0.001$ .
**Table 7.** Variance analysis of the regression model for the response surface on the latex flow rate.

Source	Sum of Squares	df	Mean Square	F-Value	p-Value	Level of Significance
Model	104.78	9	11.64	14.3	0.0001	***
A (vertical blade height)	67.93	1	67.93	83.44	<0.0001	***
B (cutting force)	5.68	1	5.68	6.97	0.0247	*
C (spiral angle)	9.44	1	9.44	11.6	0.0067	**
AB	7.8	1	7.8	9.58	0.0113	*
AC	0.4513	1	0.4513	0.5543	0.4737	-
BC	4.96	1	4.96	6.09	0.0332	*
A <sup>2</sup>	7.61	1	7.61	9.35	0.0121	*
B <sup>2</sup>	0.1075	1	0.1075	0.132	0.7239	-
C <sup>2</sup>	0.8972	1	0.8972	1.1	0.3185	-
Residual	8.14	10	0.8142			
Lack of fit	5.79	5	1.16	2.47	0.1721	-
Pure error	2.35	5	0.4697			
Cor total	112.92	19				

 $R^2 = 0.93; R^2_{adj} = 0.86; R^2_{pre} = 0.58$ 
 $R^2$  = coefficient of determination,  $R^2_{adj}$  = adjusted  $R^2$ ,  $R^2_{pre}$  = predicted  $R^2$ . Level of significance \*\*\*  $p < 0.001$ , \*\*  $p < 0.01$ , \*  $p < 0.05$ .
**Table 8.** Variance analysis of regression model for the response surface on average cutting current.

Source	Sum of Squares	df	Mean Square	F-Value	p-Value	Level of Significance
Model	0.3311	9	0.0368	2.47	0.0872	-
A (vertical blade height)	0.0192	1	0.0192	1.29	0.282	-
B (cutting force)	0.1206	1	0.1206	8.11	0.0173	*
C (spiral angle)	0.017	1	0.017	1.14	0.3105	-
AB	0.0512	1	0.0512	3.44	0.0931	-
AC	0.0128	1	0.0128	0.8612	0.3753	-
BC	0.0005	1	0.0005	0.0303	0.8653	-
A <sup>2</sup>	0.0102	1	0.0102	0.6857	0.427	-
B <sup>2</sup>	0.0237	1	0.0237	1.6	0.235	-
C <sup>2</sup>	0.0687	1	0.0687	4.62	0.0571	-
Residual	0.1486	10	0.0149			
Lack of fit	0.0693	5	0.0139	0.8731	0.5574	-
Pure error	0.0793	5	0.0159			
Cor total	0.4797	19				

 $R^2 = 0.69; R^2_{adj} = 0.41; R^2_{pre} = -0.36$ 
 $R^2$  = coefficient of determination,  $R^2_{adj}$  = adjusted  $R^2$ ,  $R^2_{pre}$  = predicted  $R^2$ . Level of significance \*  $p < 0.05$ .

The non-significant value of the lack of fit ( $p = 0.54, p > 0.05$ ) showed that the model was fitted with good prediction ( $R^2 = 0.95$ ) (shown in Table 6). Various factors showed a significant effect on cutting time. These were linear (B) and quadratic ( $B^2$ ) effects. The cutting force (B) produced the maximum effect on cutting time. Based on the F test result, the impact order showed cutting force (B) > spiral angle (C) > vertical blade height (A).

The non-significant value of the lack of fit ( $p = 0.17, p > 0.05$ ) showed that the model was fitted with good prediction ( $R^2 = 0.93$ ) (shown in Table 7). Various factors showed a significant effect on the latex flow rate. These were linear (A, B, C), interactive (AB, BC), and quadratic ( $A^2$ ) effects. The vertical blade height (A) produced the maximum effect on the latex flow rate. Based on the F test result, the impact order showed vertical blade height (A) > spiral angle (C) > cutting force (B).

The non-significant value of the lack of fit ( $p = 0.56, p > 0.05$ ) showed that the model was fitted with good prediction ( $R^2 = 0.69$ ) (shown in Table 8). Only one factor showed a significant effect on the cutting rate of the old rubber line: linear (B). The cutting force (B) produced the maximum effect on the cutting rate of the old rubber line. Based on the F test result, the impact order showed cutting force (B) > vertical blade height (A) > spiral angle (C).

### 3.3. Interaction Results for Response Surface

In order to visually and deeply analyze the interactive effects of the three factors on tapping quality and stability, Design-Expert 12 software was used to draw response surface curves. Various response surface 3D graphs for the interaction of the three factors on the tapping effect of  $Y_1, Y_2, Y_3,$  and  $Y_4$ , are shown in Figures 7–9, respectively.

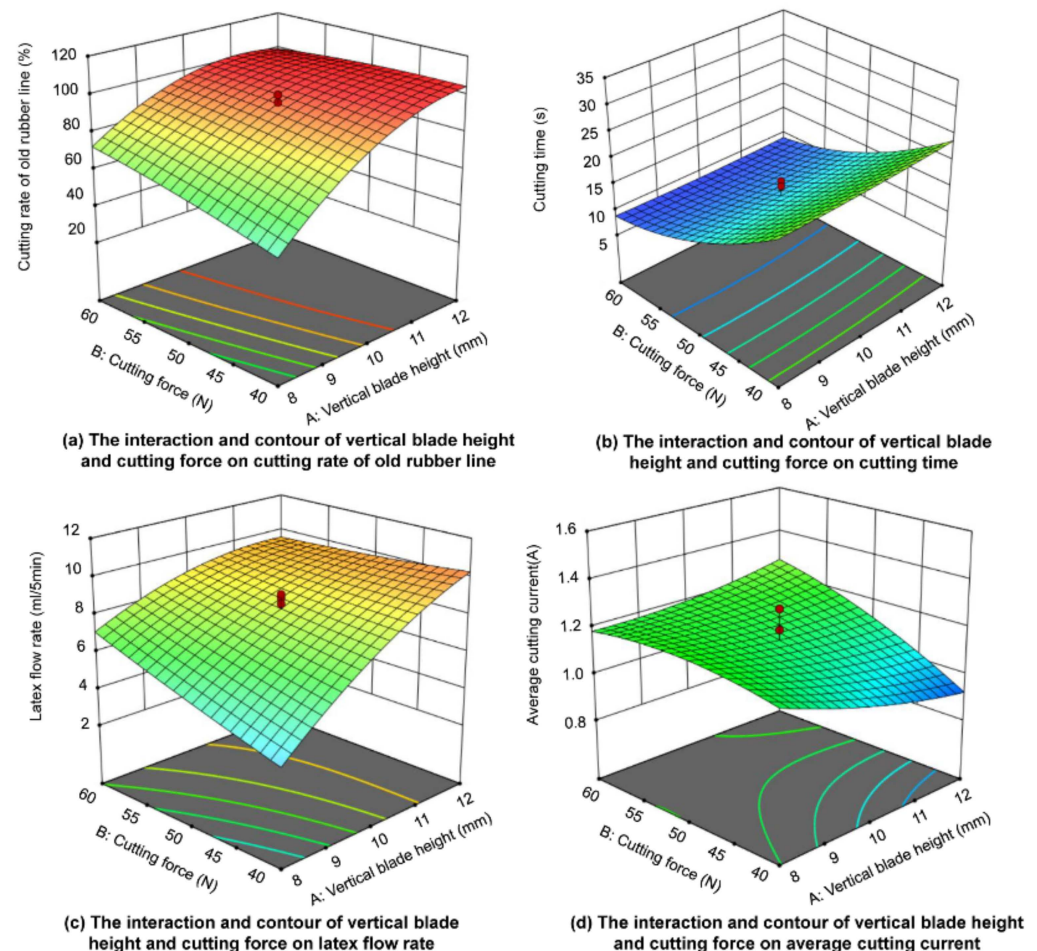


**Figure 7.** Various response surface 3D graphs for the interaction of vertical blade height (A) and cutting force (B) on the tapping effect.

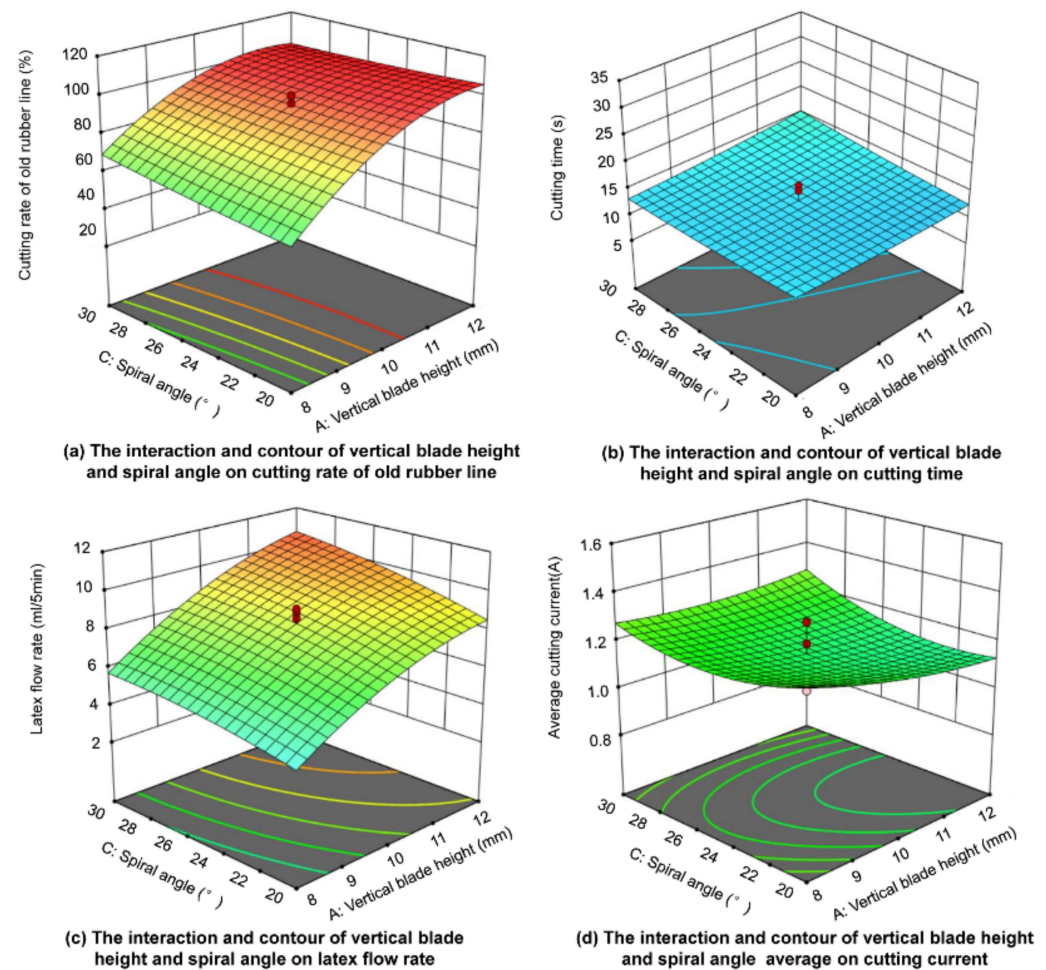


**Figure 8.** Various response surface 3D graphs for the interaction of vertical blade height (A) and spiral angle (C) on the tapping effect.

Various response surface 3D graphs were generated for the interaction of vertical blade height (A) and cutting force (B) on the tapping effect (shown in Figure 7). As the vertical blade height increased from 8 mm to 10 mm, the cutting rate of the old rubber line and latex flow rate both increased rapidly, but the cutting time and average cutting current were not significant. As the cutting force increased from 40 N to 60 N, the cutting time reduced rapidly, and the latex flow rate increased rapidly, but the cutting rate of the old rubber line and average cutting current were not significant. As the vertical blade height increased from 8 mm to 10 mm, the cutting time reduced rapidly with increasing cutting force. This indicated that the vertical blade height had a significant effect on the cutting rate of the old rubber line and latex flow rate, and the cutting force had a significant effect on the cutting time. This was consistent with the previous analysis of variance.

Various response surface 3D graphs were generated for the interaction of vertical blade height (A) and spiral angle (C) on the tapping effect (shown in Figure 8). As the spiral angle increased from 20° to 40°, the latex flow rate increased rapidly, but the cutting rate of the old rubber line, cutting time, and average cutting current were not significant. As the vertical blade height increased from 8 mm to 10 mm, the latex flow rate increased rapidly with increasing spiral angle. This indicated that the vertical blade height and spiral angle both had a significant effect on the latex flow rate. This was consistent with the previous analysis of variance.

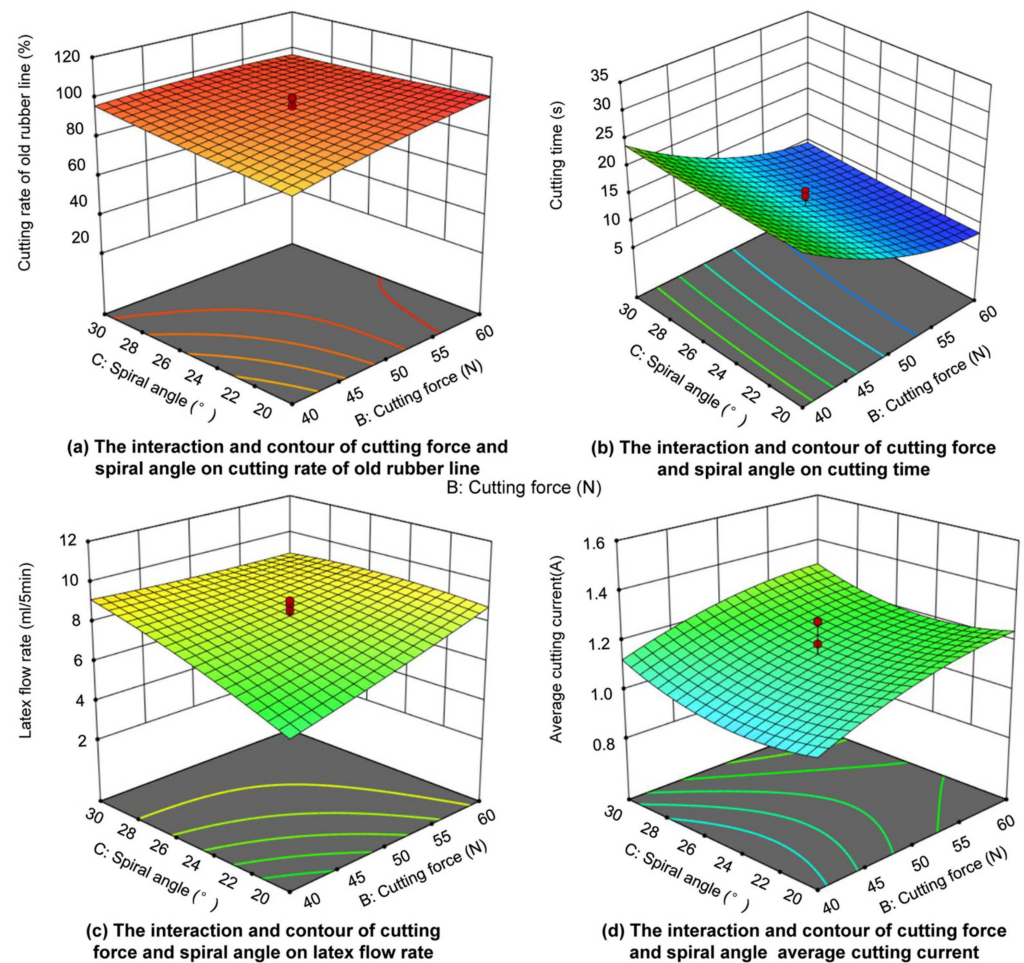


**Figure 9.** Various response surface 3D graphs for the interaction of cutting force (B) and spiral angle (C) on the tapping effect.

Various response surface 3D graphs were generated for the interaction of cutting force (B) and spiral angle (C) on the tapping effect (shown in Figure 9). As the cutting force increased from 40 N to 60 N, the cutting time reduced rapidly with increasing cutting force, but the cutting rate of the old rubber line, cutting time, and average cutting current were not significant. As the spiral angle increased from 20° to 40°, the latex flow rate increased rapidly with increasing cutting force. This indicated that the cutting force had a significant effect on the cutting rate of the old rubber line and latex flow rate, and the spiral angle had a significant effect on the cutting rate of the old rubber line. This was consistent with the previous analysis of variance.

### 3.4. Model Verification Test

Under optimal conditions, the influencing factors of A, B, and C were 10.24 mm, 51.67 N, and 24.77°, respectively, when the evaluation index values of  $Y_1$ ,  $Y_2$ ,  $Y_3$ , and  $Y_4$  were 98%, 8.65 mL/5 min, 9.00 s, and 1.16 A. The range of the relative error between the experimental and predicted results was between −11.11% and 11.11% (shown in Table 9). The measured parameters were determined to match the expected values. The results revealed that the regression equation accurately described the scenario, demonstrating conclusively that the chosen model was reasonable. The results showed that mechanical tapping could be optimally achieved using the response surface method.

Table 9. Model verification test results.

Test Number	Cutting Rate of the Old Rubber Line (%)	Relative Error/%	Latex Flow Rate (mL/5 min)	Relative Error/%	Cutting Time (s)	Relative Error/%	Average Cutting Current (A)	Relative Error/%
1	100	2.04	9.10	5.20	10.00	11.11	1.19	2.59
2	96	−2.04	8.80	1.73	8.00	−11.11	1.24	6.45
3	95	−3.06	9.40	8.67	10.00	11.11	1.23	6.03
Predicted value	98	-	8.65	-	9.00	-	1.16	-

### 3.5. Comparison Test

Compared to a V-shape pushing type tapping tool, the mechanical cutter was also able to successfully finish the entire rubber tapping operation; the tapping panel after rubber tapping was also clean and smooth, and the tapping effect was better (shown in Figure 10). Cutting with a mechanical cutter was relatively stable and satisfies the requirements for rubber tapping operations. The mechanical tapping method improved the cutting efficiency, practicality, and operability of rubber tapping.

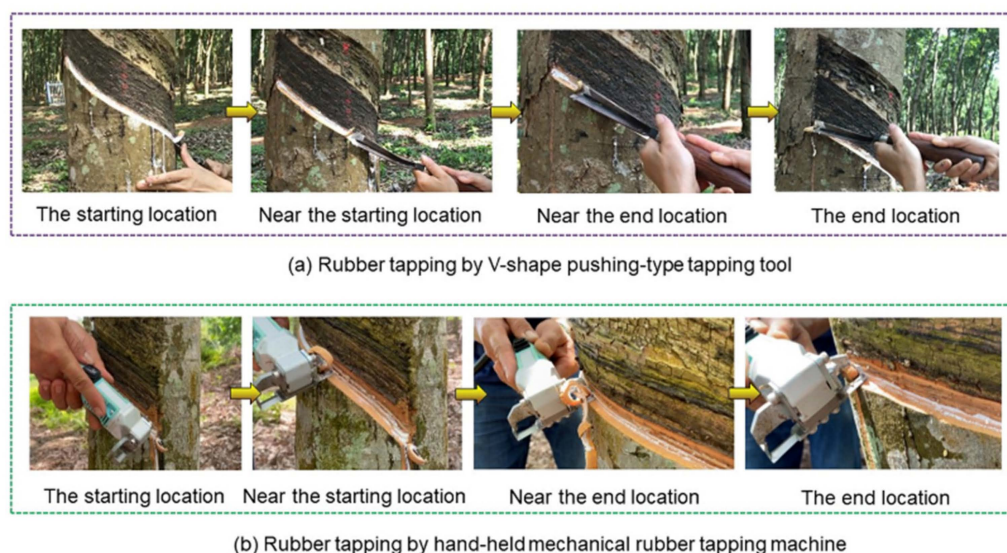
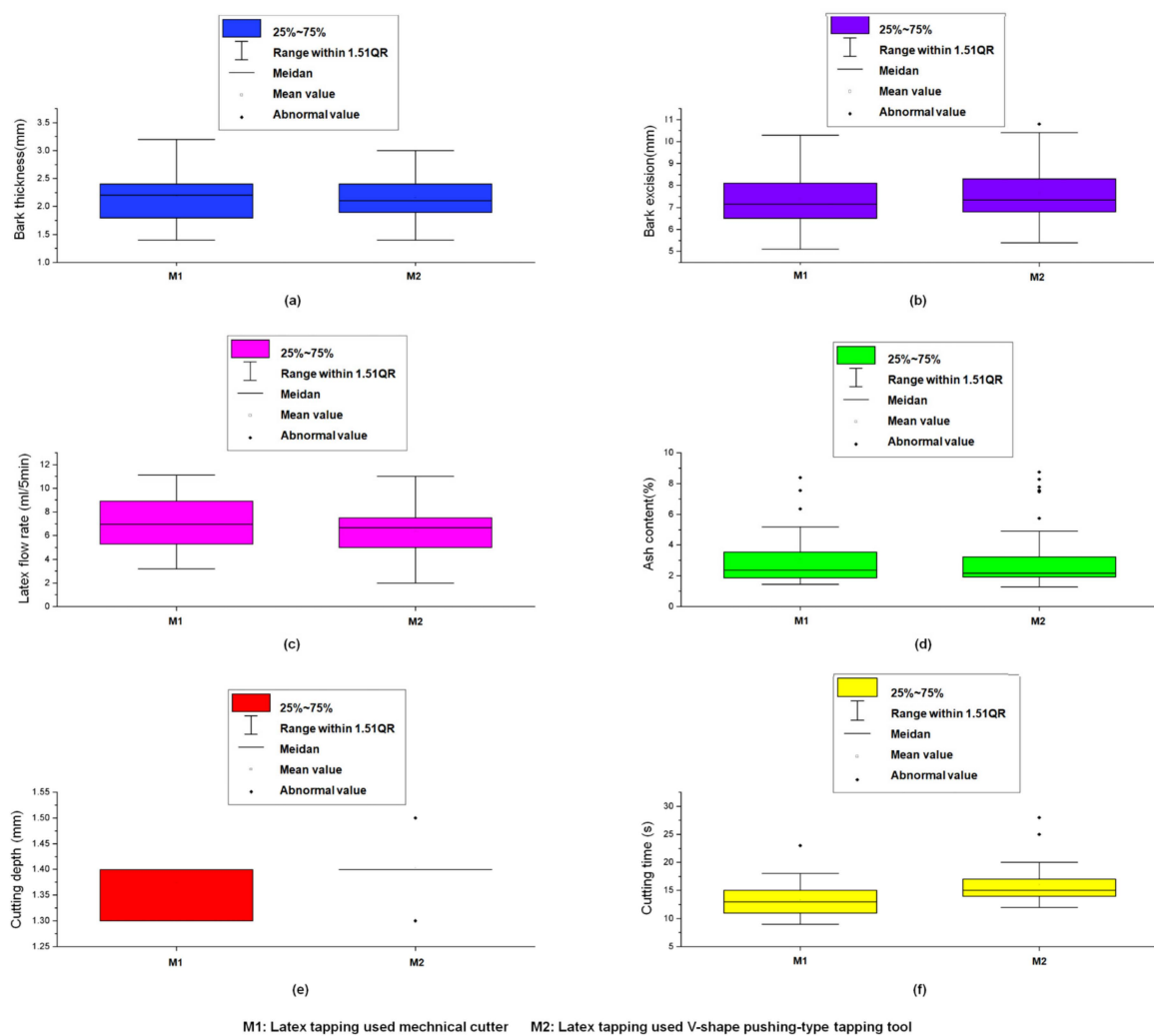


Figure 10. Rubber tapping with the two tapping tools.

The average bark thickness, average bark excision, average latex certain velocity, average ash content, average cutting depth, and average cutting time using hand and mechanical tapping methods were 2.16 mm and 2.19 mm, 7.70 mm and 7.43 mm, 6.40 mL/5 min and 7.00 mL/5 min, 3.28% and 3.08%, 1.37 mm and 1.40 mm, and 16.10 s and 13.33 s, respectively (shown in Figure 11). There was no significant difference between the two tapping methods, except ash content ( $p < 0.05$ ) and cutting time ( $p < 0.01$ ) (shown in Table 10).

Compared to a V-shape pushing type tapping tool, bark thickness had an average variation rate of 7.55%, and bark consumption had an average fluctuation rate of 3.62%. Bark thickness was relatively smaller, resulting in a slightly larger cutting depth. The mechanical cutter increased the average latex flow rate by 9.38%, indicating that it was more conducive to rubber discharge. The mechanical cutter significantly reduced the cutting time by 17.20%, indicating that it was faster in a single rubber tree tapping. The ash content increased by 6.10% but was slightly lower, indicating that mechanical tapping did not contaminate the latex. The cutting depth increased significantly by 21.90%, indicating a greater distance from the cambium and perhaps less possible tree injury.



**Figure 11.** Comparison of the tapping effects of 30 rubber trees between hand and mechanical tapping methods: (a) bark thickness, (b) bark excision, (c) latex flow time, (d) cutting time, (e) ash content, (f) cutting depth.

**Table 10.** The *t*-test analysis of tapping effects.

Source	Mean Value 1	Mean Value 2	Mean Standard Error 1	Mean Standard Error 2	df	<i>t</i> -Value	<i>p</i> -Value	Level of Significance
Bark thickness	2.16	2.19	0.072	0.090	58	0.262	0.795	-
Bark excision	7.43	7.70	0.23	0.22	58	-0.843	0.403	-
Latex flow time	6.97	6.39	0.40	0.39	58	1.028	0.308	-
Cutting time	13.33	16.10	0.62	0.62	58	-3.154	0.003	**
Ash content	3.08	3.28	0.33	0.42	58	-0.373	0.710	-
Cutting depth	1.40	1.37	<0.01	0.01	58	-2.298	0.025	*

Level of significance \*\*  $p < 0.01$ , \*  $p < 0.05$ . Mean value 1 and mean standard error 1: latex tapping using the mechanical method. Mean value 2 and mean standard error 2: latex tapping using the hand tapping method.

After the hand-held mechanical rubber tapping machine entered a stable state or the no-load current stabilized at 0.029 A, the cutting test began. Among the thirty cutting test results, there were five discontinuous trees, which accounted for approximately 20% of the total test sample trees (shown in Figure 12). This indicated that the cutting stability of the blade and guide using the cutter reached 80%, which satisfied the requirements for rubber tapping operations. All cutting currents except for group (d) did not show a no-load current of 0.029 A, indicating a continuous cutting process.

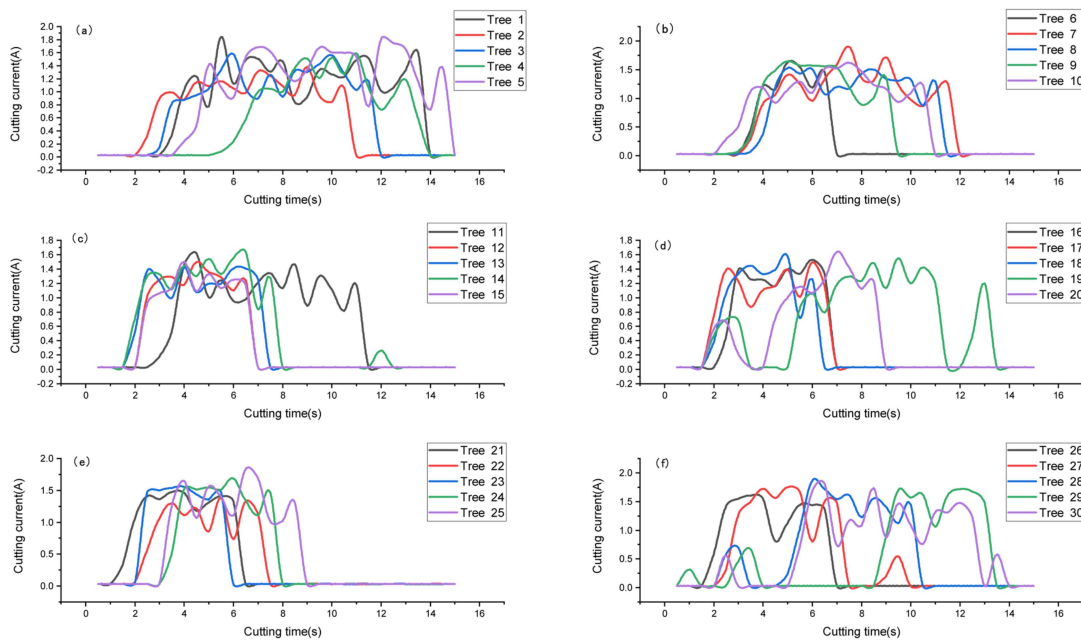


**Figure 12.** The waveform diagrams of the cutting current of 30 rubber trees during rubber tapping: (a) trees 1–5, (b) 6–10, (c) 11–15, (d) 16–20, (e) 21–25, and (f) 26–30.

During the mechanical rubber tapping process, the maximum and minimum cutting currents fluctuated due to load influences but were generally stable (shown in Figure 13). In a single-cutting process, the minimum cutting current was greater than the no-load current, and the average cutting current was greater than the minimum cutting current but less than the maximum cutting current. The no-load current remained stable at 0.029 A, the average cutting current was essentially stable between 1.0 and 1.5 A, and the maximum cutting current was less than 2.0 A, close to 1.5 A. Cutting with a mechanical cutter was relatively stable and satisfies the requirements for rubber tapping operations.

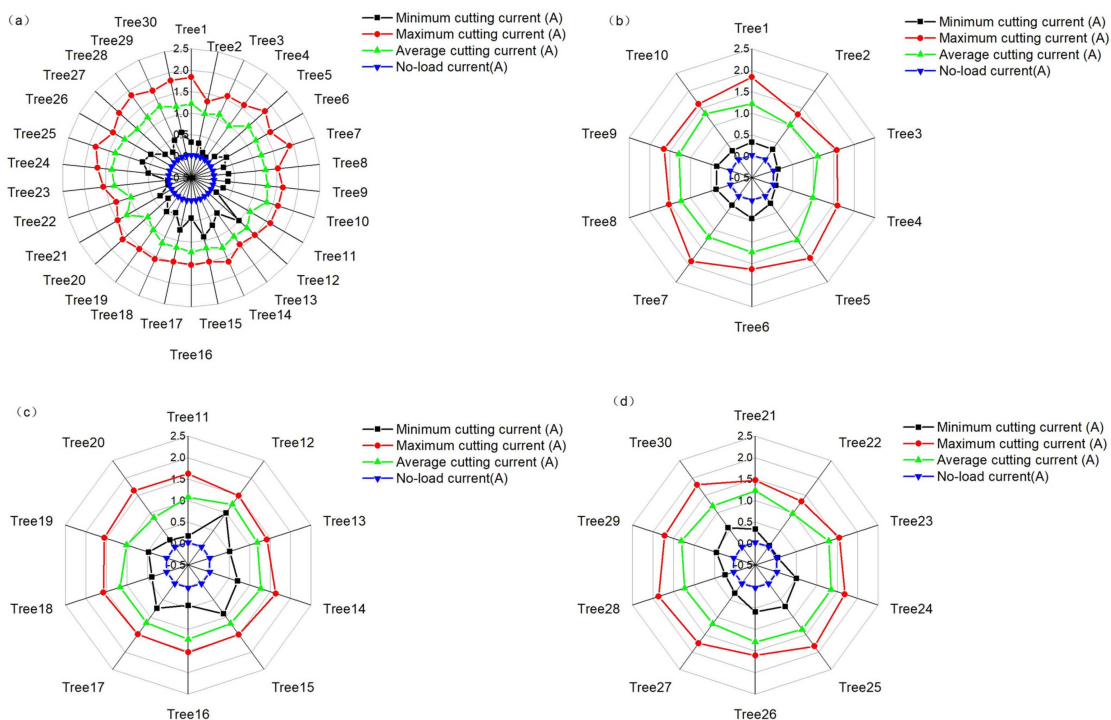


**Figure 13.** Cutting current stability in rubber tapping: (a) trees 1–30, (b) 1–10, (c) 11–20, (d) 21–30.

## 4. Discussion

In the current study, we hypothesized that the mechanical cutting machine with a blade and guide could easily strip old rubber lines from rubber trees, as well as improve the cutting efficiency and operability of rubber tapping. These hypotheses were supported by the results from our investigation, adopting the evaluation methods of the single-factor test, response surface optimization test, and comparison test. Therefore, in this study, a novel hand-held mechanical rubber tapping machine would be an effective and operable promising measure to promote the sustainable production of natural rubber.

### 4.1. Feasibility of the Mechanic Cutter

Agricultural machinery is crucial to achieve cost savings, quality improvement, and efficiency enhancement in agriculture. This technology has been used to mechanize a variety of crops, including wheat, corn, rice, and peanuts [47–49]. Large-scale rubber tree planting has been ongoing for more than a century, and conventional methods of cutting rubber panels still rely on manual labor using manpower to push or pull knives. Due to the high elasticity of the old rubber line left over after rubber tapping, it should be physically removed before the next rubber tapping. Rubber trees are effectively grown in China and are continuously tapped by V-shaped pushing type tapping tools. Rubber tapping is considered to be a skill-oriented job and relies on manpower completely. The decline in skilled rubber tappers, low income from rubber, and increased labor charges have become increasingly significant issues in rubber production [16–19]. Rubber tapping machines are urgently needed [19].

Is tapping with a mechanic knife feasible? Firstly, it is powered by a battery. Rubber tapping workers only need to hold the handle shank and pull the machine along the tapping line easily in rubber tapping. Secondly, rubber tapping workers without technical experience can be trained to master the machine correctly in 3–5 days. The machine is more suited for new rubber tapping workers. Thirdly, the tapping machine settings could be adjusted to match specific tree anatomy. By changing the distance between the guide and blade, the cutting depth and bark thickness could be adjusted. Compared to a V-shape pushing type tapping tool, the tapping panel after rubber tapping was also clean and smooth, and the tapping effect was better. Fourthly, a vertical blade with a 10 mm height could excise the old rubber line easily and improve quality and was first applied in the field of rubber tree harvesting. Fifthly, cutting depth in this study could potentially significantly increase or reduce tree damage. The tapping panel after rubber tapping is clean and smooth. Compared to a V-shape pushing type tapping tool, a mechanical cutter could be used more easily and efficiently used by workers after simple training. According to the specifications of standards NY/T1088-2006 and NY/T267-2006 in China, the tapping quality of the new tapping machine in this study is comparable to the traditional tapping knife.

In the test, 30 sample trees are selected to verify the prototyping test with the optimized treatment scheme. Further validation is needed for large-scale applications in future research. A tapping task is usually made of 500 to 700 trees and is completed in 3–4 h using a traditional tapping knife. According to saving 3–5 s per tree, a tapping task could save 0.41–0.95 h using a hand-held mechanical tapping machine in theory. The characteristics of being easy to carry and having a low cost and simple maintenance make the mechanical tapping machine more feasible. But, there are still a lot of questions on the feasibility of mechanical tapping in field tapping tasks, including battery autonomy, occupational disease, machine faults, mechanical vibration, and noise. Further validation is needed for large-scale applications in future research. The new hand-held tapping machine could be used by workers after simple training. It has a good effect on raising farmers' income and reviving the rural economy because it not only reduces time and labor costs but also frees up some labor to work in other enterprises. If it is applied on a large scale, the novel tapping machine could reduce physical demands, decrease reliance on skilled workers, and make tapping machines more practical and operable.

#### 4.2. Optimization of the Mechanic Cutter

The experimental scheme and research method are credible and feasible. Calculations are made to determine the factors, blade parameters, and force analysis. The main certified factors are cutting force, vertical blade height, spiral angle, and the angle of the blade edge. According to traditional reliability data, the range of the spiral angle and the value of the blade edge are 20–30° and 4°, respectively. To determine the range of cutting force and vertical blade height for response surface optimization, a single-factor test is designed. The range of cutting force and vertical blade height are 8–12 mm and 40.00–60.00 N, respectively. Based on the calculation and single-factor results, the response surface method (RSM) and the center combined rotation design (CCRD) optimization method are adopted to explore the influence of three influencing factors of vertical blade height (A), cutting force (B), and spiral angle (C). The values of the old rubber line ( $Y_1$ ), cutting time ( $Y_2$ ), latex flow rate ( $Y_3$ ), and average cutting current ( $Y_4$ ) are regarded as evaluation indexes of the tapping effect. The quadratic model fits for all the responses. The experimental values are in close agreement with the predicted values.

Compared to the V-shaped blade and circular saw blade, the blade with only a horizontal edge is commonly applied in mechanical rubber tapping machines [13,19,22,45,46]. The mechanical cutter with vertical blade height has been designed and optimized in this study. It can help excise old rubber lines easily and save cutting time. The optimization of cutting force can help reduce mechanical wear and rubber tree damage. The optimization of the spiral angle can help design tapping lines and stabilize latex production. To verify the availability and effect of the mechanical tapping method preliminarily, a comparison test between hand and mechanical tapping tools is designed, and only 30 sample trees with good old rubber lines are selected. Six important evaluation indexes of rubber production are selected, including bark thickness, bark excision, latex flow time, cutting time, ash content, and cutting depth. The research has great significance in providing theoretical support for further relevant research.

The bark comprises a water capsule skin, yellow skin, an inner layer of sand skin, an outer layer of sand skin, and coarse skin from the inside to the outside. The primary section of the bark that produces rubber is the yellow bark. However, damage to the water capsule skin will diminish latex yield. In future studies, we also can attempt to use the ultrasound-assisted extraction method to examine the characteristics of latex production [50–55]. It was also important to take into consideration using various rubber tree and machine species as test subjects in further research [56,57]. With the advancement of information technology, rubber tapping intelligent technologies mainly include tapped area detection and new tapping line location [29], object detection algorithm [58], rubber-tapped path detection, nighttime rubber tapping line detection [11,59], rubber tapping robot forest navigation, and information collection systems [13,22]. One tendency in rubber tapping advancement is the fusion of mechanical cutters and intelligent technology advantages.

#### 4.3. Applicability

Mechanical cutting machines are gradually used in rubber tree tapping, including hand-held electrical tapping knives [19,60], fixed tapping machines, and self-propelled rubber tapping robots [13,19,22]. These might allow some rubber tapping workers to become free to work in other industries and raise the family incomes. Currently, most mechanical tapping machines are still in the laboratory stage and have not yet reached the stage of industrialization and commercial use [19,22]. Although the hand-held rubber tapping machine has made significant development, rubber tapping employees are only just beginning to accept it. Using modern machinery, it is still more challenging to entirely strip thick old rubber lines.

In key rubber-producing nations, like China, Vietnam, Thailand, India, Sri Lanka, Myanmar, Laos, Cambodia, Malaysia, and Indonesia, over 10,000 machines with the new mechanical cutter have been promoted and put to use. This technology has advanced to a preeminent level on the global stage and has been chosen as a key piece of machinery

for China's rural and agricultural areas. It is anticipated that the new mechanical cutting technique will be successfully used in intelligent rubber tapping machinery, such as self-propelled rubber tapping robots and fixed automatic tapping machines. We also anticipate that the mechanical cutter's promotion will lead to further uses for related products in the future.

## 5. Conclusions

To enhance cutting effectiveness, quality, and operability, a thorough investigation of mechanical cutting technology using the blade and guide is very important. The optimization of the mechanical rubber cutting strategy was successfully examined using response surface methodology. This was the first report on the optimization of the mechanical rubber cutting strategy for rubber tree harvesting. The optimized condition was validated and was in close agreement with experimental values. This outcome suggested the following:

- (1) A mechanical rubber tapping mechanism with a vertical blade and an adjustable guide was first proposed. The mechanism involved with a 10 mm vertical blade height could excise old rubber lines easily and improve quality and was first applied in the field of rubber tree harvesting.
- (2) Based on the single-factor results, the response surface method (RSM) and the center combined rotation design (CCRD) optimization method were adopted to explore the influence of three influencing factors on the tapping effect. The influencing sequence of three factors on the four response values of  $Y_1$ ,  $Y_2$ ,  $Y_3$ , and  $Y_4$  was as follows:  $A > B > C$ ,  $B > C > A$ ,  $A > C > B$ , and  $B > A > C$ , respectively. Under optimal conditions, the influencing factors of A, B, and C were 10.24 mm, 51.67 N, and  $24.77^\circ$ , respectively, when the evaluation index values of  $Y_1$ ,  $Y_2$ ,  $Y_3$ , and  $Y_4$  were 98%, 8.65 mL/5 min, 9.00 s, and 1.16 A.
- (3) Using a blade with a height of more than 10 mm was not necessary to manually tear the old rubber lines prior to rubber tapping. The old rubber line might be removed using a blade with a height of 10 mm and a cutting rate of more than 95%. However, a thorough analysis based on the two factors of processing expense and technical challenge revealed that blades with a height of 10 mm demonstrated superior cost-effectiveness and were taken into consideration for selection in rubber tapping.
- (4) In a comparison test between two tapping tools, there was no significant difference between hand and mechanical methods, except ash content ( $p < 0.05$ ) and cutting time ( $p < 0.01$ ), suggesting a potential reduction in tree damage and cutting faster in single rubber tree tapping. The no-load current was stable at 0.029 A, the average cutting current was stable between 1.0 and 1.5 A, and the maximum cutting current was less than 2.0 A, close to 1.5 A.

In general, a novel, hand-held mechanical rubber tapping machine was described. The response surface method was applied to evaluate factors affecting the tapping effect. The experimental values were in close agreement with the predicted value. Machine-tapped latex was comparable in quality to hand-tapped latex. We recommend that if the mechanical tapping machine is widely applied in rubber harvesting, it will help reduce the physical demands, decrease reliance on skilled workers, and improve tapping efficiency, practicality, and operability. Furthermore, it provides crucial theoretical references for the development of intelligent tapping machines.

**Author Contributions:** Conceptualization, L.W., Y.Z. and J.H.; methodology, L.W., Y.Z. and J.H.; software, L.W., Y.Z. and J.H.; validation, L.W., Y.Z. and J.H.; formal analysis, L.W. and C.H.; investigation, T.L. and J.C.; resources, L.W.; data curation, L.W. and J.H.; writing—original draft preparation, L.W.; writing—review and editing, L.W., Y.Z. and J.H.; visualization, T.L. and C.H.; supervision, Y.Z. and J.H.; project administration, L.W.; funding acquisition, L.W., Y.Z. and J.H. All authors have read and agreed to the published version of the manuscript.

**Funding:** This research was funded by the Hainan Provincial Natural Science Foundation of China, No. 522RC788 (L.W.), and the National Key R&D Program of China, No. 2020YFD1000602-9 (L.W.).

**Data Availability Statement:** Data are contained within the article.

**Acknowledgments:** All authors would like to express their utmost gratitude to contributions from Lifeng Wang, Huichuan Jiang, Bo Fan, Feng An, and Yunqing Han. We especially thank all research subjects for their assistance and participation in this study.

**Conflicts of Interest:** The authors declare no conflict of interest.

## Appendix A

**Mechanical cutter.** A mechanical cutter was designed using adjustable guides and cutting blades (shown in Figure A1). The side of the guide was aligned with the cut surface, and the end of the guide was in point contact with the inner side of the tapping line of the rubber tree. The mechanical cutter was loaded onto the front end of a hand-held mechanical rubber tapping machine and conducted experiments on rubber tapping. Rubber tapping involves the use of an adjustable guide and a blade. Between the guide and blade, the space could be continually changed in all directions—forward, back, up, and down. By changing the distance between the two, the cutting depth and bark thickness could be adjusted.

**Operating instruction.** The hand-held mechanical rubber tapping machine mainly includes a hand shank, mechanical cutter, battery, lumbar bag, and power connection cable. Firstly, put on the lumbar bag and keep the battery in the lumbar bag. Secondly, hold the hand shank with one hand, turn on the on–off button, and pull the mechanical machine along the tapping line. The tapping worker should move the machine from top to bottom or bottom to top along the tapping line until the rubber tapping is finished. It also can be used by a traditional tapping method without power.

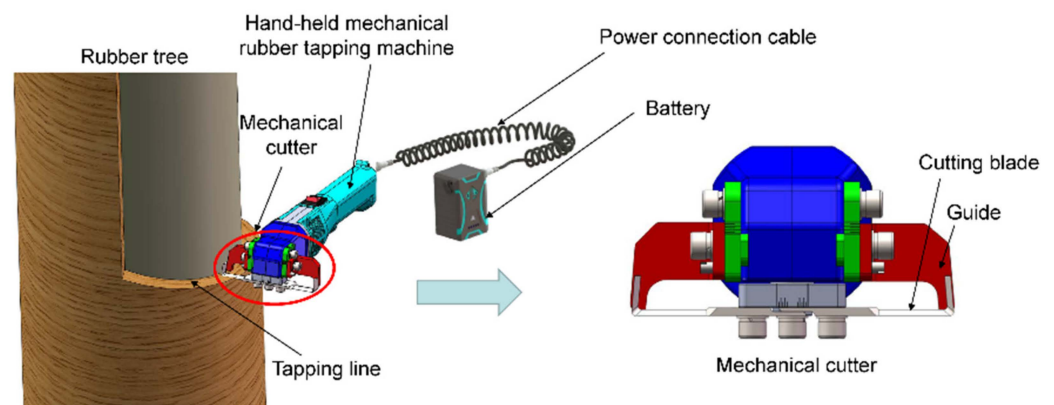


**Figure A1.** Mechanical cutter with adjustable guide and cutting blade.

## Appendix B

**Blade parameters and force analysis.** The rubber tapping blade parameters and force analysis are shown in Figure A2. According to Lagrange theorem, the force of the rubber cutting blade should satisfy the following conditions in rubber tapping:

$$\begin{cases} F \cos \beta - F_{f1} - F_{n2} \cos(\theta - \beta) - (G + F_{f2}) \sin(\theta - \beta) \geq 0 \\ F_{n1} + F_1 + F \sin \beta - F_{n2} \sin(\theta - \beta) - (G + F_{f2}) \cos(\theta - \beta) = 0 \\ F_{f1} = \mu F_{n1} \\ F_{f2} = \mu F_{n2} \\ F_1 = mR\omega^2 \\ \mu = \tan \delta \end{cases} \quad (\text{A1})$$

where:

- $F$ —cutting force, expressed in N;
- $F_1$ —rotational centrifugal force generated by blade motion, expressed in N;
- $F_{n1}$ —reaction on the horizontal blade, expressed in N;

- $F_{n2}$ —reaction on the vertical blade, expressed in N;
- $G$ —blade gravity, expressed in N;
- $F_{f1}$ —friction force on the horizontal blade, expressed in N;
- $F_{f2}$ —friction force on the vertical blade, expressed in N;
- $m$ —blade mass, expressed in g;
- $v$ —blade cutting speed in rubber tapping, expressed in m/s;
- $\beta$ —angle of the blade edge, expressed in degree ( $^{\circ}$ );
- $\delta$ —friction angle between the blade and rubber trunk, expressed in degree ( $^{\circ}$ );
- $\mu$ —friction factor between the blade and rubber trunk.

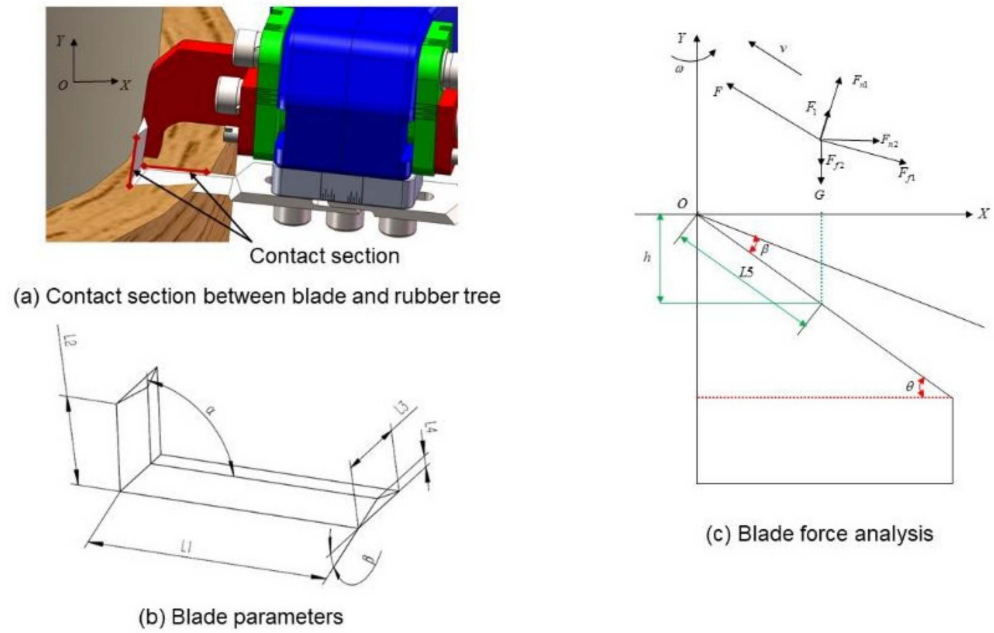


Figure A2. Blade parameters and force analysis.

According to the blade parameters (Figure 5b) and geometric relationship (Figure 5c), relation equations were as follows:

$$\begin{cases} \sin \beta = \frac{L_4}{\sqrt{\left(\frac{L_3}{2}\right)^2 + L_4^2}} = \frac{2L_4}{\sqrt{L_3^2 + 4L_4^2}} \\ \cos \beta = \frac{\left(\frac{L_3}{2}\right)^2}{\sqrt{\left(\frac{L_3}{2}\right)^2 + L_4^2}} = \frac{L_3^2}{2\sqrt{L_3^2 + 4L_4^2}} \\ \sin(\theta - \beta) = \frac{h}{L_5} \\ \cos(\theta - \beta) = \frac{\sqrt{L_5^2 - h^2}}{L_5} \end{cases} \quad (A2)$$

where:

- $L_1$ —length of the horizontal blade, expressed in mm;
- $L_2$ —height of the vertical blade, expressed in mm;
- $L_3$ —blade width, expressed in mm;
- $L_4$ —blade thickness, expressed in mm;
- $L_5$ —blade contact length in rubber tapping, expressed in mm;
- $h$ —blade contact height in rubber tapping, expressed in mm;
- $\alpha$ —the angle between the horizontal and vertical blade, expressed in degree ( $^{\circ}$ ).

The simplified formula of equation set (18) is as follows:

$$\begin{cases} F_{f1} = F_{f2}[\sin(\theta - \beta) + \tan \delta \cos(\theta - \beta)] + \tan \delta [G \cos(\theta - \beta) - mR\omega^2 - F \sin \beta] \\ F_{f2} \leq \frac{F(\cos \beta - \tan \delta \sin \beta) - G(1 + \tan \delta)[\sin(\theta - \beta) + \cos(\theta - \beta)] - mR\omega^2 \tan \delta}{(\tan \delta + \frac{1}{\tan \delta}) \cos(\theta - \beta) + 2 \sin(\theta - \beta)} \end{cases} \quad (A3)$$

According to equation sets (19) and (20), relation equations are calculated as follows:

$$\begin{cases} F_{f1} = F_{f2} \frac{h + \tan \delta \sqrt{L_5^2 - h^2}}{L_5} + \tan \delta \left[ G \frac{\sqrt{L_5^2 - h^2}}{L_5} - mR\omega^2 - F \frac{2L_4}{\sqrt{L_3^2 + 4L_4^2}} \right] \\ F_{f2} \leq \frac{FL_5 \tan \delta \left( \frac{L_3^2}{2\sqrt{L_3^2 + 4L_4^2}} - \tan \delta \frac{2L_4}{\sqrt{L_3^2 + 4L_4^2}} \right) - mR\omega^2 L_5 \tan^2 \delta}{(1 + \tan \delta)(\sqrt{L_5^2 - h^2} + 2h)} - \frac{G \tan \delta (h + \sqrt{L_5^2 - h^2})}{\sqrt{L_5^2 - h^2} + 2h} \end{cases} \quad (A4)$$

According to equation set (6), the main factors of the blade friction forces ( $F_{f1}$  and  $F_{f2}$ ) are cutting force ( $F$ ), friction angle between the blade and rubber trunk ( $\delta$ ), spiral angle ( $\theta$ ), and angle of the blade edge ( $\beta$ ). In the common traditional method of hand rubber tapping, the spiral angle was 20–30°, and the angle of the blade edge was 4°.

## References

- Dakin, M.J.; Yentis, S.M. Latex allergy: A strategy for management. *Anaesthesia* **1998**, *53*, 774–781. [[CrossRef](#)] [[PubMed](#)]
- She, F.; Zhu, D.; Kong, L.; Wang, J.; An, F.; Lin, W. Ultrasound-assisted tapping of latex from Para rubber tree *Hevea brasiliensis*. *Ind. Crops Prod.* **2013**, *50*, 803–808. [[CrossRef](#)]
- Chambon, B.; Duangta, K.; Promkhambut, A.; Lesturgez, G. Field latex production in Southern Thailand: A study on farmers' and traders' practices that may affect the quality of natural rubber latex delivered to the factories. *J. Rubber Res.* **2020**, *23*, 125–137. [[CrossRef](#)]
- Men, X.; Wang, F.; Chen, G.-Q.; Zhang, H.-B.; Xian, M. Biosynthesis of natural rubber: Current state and perspectives. *Int. J. Mol. Sci.* **2019**, *20*, 50. [[CrossRef](#)] [[PubMed](#)]
- Stankevitz, K.; Schoenfish, A.; de Silva, V.; Tharindra, H.; Stroo, M.; Ostbye, T. Prevalence and risk factors of musculoskeletal disorders among Sri Lankan rubber tappers. *Int. J. Occup. Environ. Health* **2016**, *22*, 91–98. [[CrossRef](#)]
- Stankevitz, K.; Staton, C.; Schoenfish, A.; de Silva, V.; Tharindra, H.; Stroo, M.; Ostbye, T. Prevalence of occupational injury and its contributing factors among rubber tappers in Galle, Sri Lanka. *Int. J. Occup. Environ. Health* **2016**, *22*, 333–340. [[CrossRef](#)] [[PubMed](#)]
- Deng, X.; Guo, D.; Yang, S.; Shi, M.; Chao, J.; Li, H.; Peng, S.; Tian, W. Jasmonate signalling in the regulation of rubber biosynthesis in laticifer cells of rubber tree, *Hevea brasiliensis*. *J. Exp. Bot.* **2018**, *69*, 3559–3571. [[CrossRef](#)]
- Michels, T.; Eschbach, J.-M.; Lacote, R.; Benneveau, A.; Papy, F. Tapping panel diagnosis, an innovative on-farm decision support system for rubber tree tapping. *Agron. Sustain. Dev.* **2012**, *32*, 791–801. [[CrossRef](#)]
- Lima Gouvea, L.R.; Teixeira de Moraes, M.L.; Piffer Goncalves, E.C.; de Moraes, M.A.; Goncalves, P. Genetic variability of traits of the laticiferous system and association with rubber yield in juvenile and adult rubber tree progenies. *Ind. Crops Prod.* **2022**, *186*, 115225. [[CrossRef](#)]
- Qin, Y.; Wang, J.; Fang, Y.; Lu, J.; Shi, X.; Yang, J.; Xiao, X.; Luo, X.; Long, X. Anaerobic metabolism in *Hevea brasiliensis* laticifers is relevant to rubber synthesis when tapping is initiated. *Ind. Crops Prod.* **2022**, *178*, 114663. [[CrossRef](#)]
- Wongtanawijit, R.; Khaorapapong, T. Nighttime rubber tapping line detection in near-range images near-range tapping line shadow acquisition technique with tapping line detection algorithm for automatic rubber tapping robot in nighttime. *Multimed. Tools Appl.* **2021**, *80*, 29401–29422. [[CrossRef](#)]
- Pramchoo, W.; Geater, A.F.; Tangtrakulwanich, B. Physical ergonomic risk factors of carpal tunnel syndrome among rubber tappers. *Arch. Environ. Occup. Health* **2020**, *75*, 1–9. [[CrossRef](#)] [[PubMed](#)]
- Zhang, C.; Yong, L.; Chen, Y.; Zhang, S.; Ge, L.; Wang, S.; Li, W. A rubber-tapping robot forest navigation and information collection system based on 2D LiDAR and a gyroscope. *Sensors* **2019**, *19*, 2136. [[CrossRef](#)]
- Munasinghe, E.S.; Rodrigo, V.H.L. Lifespan of rubber cultivation can be shortened for high returns: A financial assessment on simulated conditions in Sri Lankan. *Exp. Agric.* **2018**, *54*, 323–335. [[CrossRef](#)]
- Zhang, S.-X.; Wu, S.-H.; Chao, J.-Q.; Yang, S.-G.; Bao, J.; Tian, W.-M. Genome-wide identification and expression analysis of MYC transcription factor family genes in rubber tree (*Hevea brasiliensis* Muell. Arg.). *Forests* **2022**, *13*, 531. [[CrossRef](#)]
- Ali, M.F.; Akber, M.A.; Smith, C.; Aziz, A.A. The dynamics of rubber production in Malaysia: Potential impacts, challenges and proposed interventions. *For. Policy Econ.* **2021**, *127*, 102449. [[CrossRef](#)]
- Rodrigo, V.H.L.; Kudaligama, K.V.V.S.; Fernando, K.M.E.P.; Yapa, P.A.J. Replacing traditional half spiral cut by a quarter cut with Ethephon; a simple approach to solve current issues related to latex harvesting in rubber industry. *J. Natl. Sci. Found. Sri.* **2012**, *40*, 283–291. [[CrossRef](#)]

18. Rukkhun, R.; Iamsaard, K.; Sdoodee, S.; Mawan, N.; Khongdee, N. Effect of high-frequency tapping system on latex yield, tapping panel dryness, and biochemistry of young hillside tapping rubber. *Not. Bot. Horti Agrobot.* **2020**, *48*, 2359–2367. [[CrossRef](#)]
19. Yang, H.; Sun, Z.; Liu, J.; Zhang, Z.; Zhang, X. The development of rubber tapping machines in intelligent agriculture: A review. *Appl. Sci.* **2022**, *12*, 9304. [[CrossRef](#)]
20. Li, J.; Chen, Z.; Shi, H.; Yu, J.; Huang, G.; Huang, H. Ultrasound-assisted extraction and properties of polysaccharide from Ginkgo biloba leaves. *Ultrason. Sonochem.* **2023**, *93*, 106295. [[CrossRef](#)]
21. Feng, L.-Y.; Liu, J.; Gao, C.-W.; Wu, H.-B.; Li, G.-H.; Gao, L.-Z. Higher genomic variation in wild than cultivated rubber trees, *Hevea brasiliensis*, revealed by comparative analyses of chloroplast genomes. *Front. Ecol. Evol.* **2020**, *8*, 237. [[CrossRef](#)]
22. Zhou, H.; Zhang, S.; Zhang, J.; Zhang, C.; Wang, S.; Zhai, Y.; Li, W. Design, development, and field evaluation of a rubber tapping robot. *J. Field Rob.* **2022**, *39*, 28–54. [[CrossRef](#)]
23. An, F.; Cahill, D.; Rookes, J.; Lin, W.; Kong, L. Real-time measurement of phloem turgor pressure in *Hevea brasiliensis* with a modified cell pressure probe. *Bot. Stud.* **2014**, *55*, 19. [[CrossRef](#)] [[PubMed](#)]
24. An, F.; Cai, X.; Rookes, J.; Xie, G.; Zou, Z.; Cahill, D.; Kong, L. Latex dilution reaction during the tapping flow course of *Hevea brasiliensis* and the effect of Ethrel stimulation. *Braz. J. Bot.* **2015**, *38*, 211–221. [[CrossRef](#)]
25. An, F.; Lin, W.; Cahill, D.; Rookes, J.; Kong, L. Variation of phloem turgor pressure in *Hevea brasiliensis*: An implication for latex yield and tapping system optimization. *Ind. Crops Prod.* **2014**, *58*, 182–187. [[CrossRef](#)]
26. Devkota, R.; Pant, L.P.; Gartaula, H.N.; Patel, K.; Gauchan, D.; Hambly-Odame, H.; Thapa, B.; Raizada, M.N. Responsible agricultural mechanization innovation for the sustainable development of Nepal's hillside farming system. *Sustainability* **2020**, *12*, 374. [[CrossRef](#)]
27. Hui, X.H.; Sun, Y.H.; Yin, F.; Dun, W.T. Trend prediction of agricultural machinery power in China coastal areas based on grey relational analysis. *J. Coast. Res.* **2020**, *103*, 299–304. [[CrossRef](#)]
28. Belwal, T.; Dhyani, P.; Bhatt, I.D.; Rawal, R.S.; Pande, V. Optimization extraction conditions for improving phenolic content and antioxidant activity in *Berberis asiatica* fruits using response surface methodology (RSM). *Food Chem.* **2016**, *207*, 115–124. [[CrossRef](#)]
29. Chen, Y.; Zhang, H.; Liu, J.; Zhang, Z.; Zhang, X. Tapped area detection and new tapping line location for natural rubber trees based on improved mask region convolutional neural network. *Front. Plant Sci.* **2023**, *13*, 1038000. [[CrossRef](#)]
30. Danmaliki, G.I.; Saleh, T.A.; Shamsuddeen, A.A. Response surface methodology optimization of adsorptive desulfurization on nickel/activated carbon. *Chem. Eng. J.* **2017**, *313*, 993–1003. [[CrossRef](#)]
31. Gadekar, M.R.; Ahammed, M.M. Modelling dye removal by adsorption onto water treatment residuals using combined response surface methodology-artificial neural network approach. *J. Environ. Manag.* **2019**, *231*, 241–248. [[CrossRef](#)] [[PubMed](#)]
32. Karimifard, S.; Moghaddam, M.R.A. Application of response surface methodology in physicochemical removal of dyes from wastewater: A critical review. *Sci. Total Environ.* **2018**, *640*, 772–797. [[CrossRef](#)] [[PubMed](#)]
33. Kumar, M.; Dahuja, A.; Tiwari, S.; Punia, S.; Tak, Y.; Amarowicz, R.; Bhoite, A.G.; Singh, S.; Joshi, S.; Panesar, P.S.; et al. Recent trends in extraction of plant bioactives using green technologies: A review. *Food Chem.* **2021**, *353*, 129431. [[CrossRef](#)] [[PubMed](#)]
34. Makela, M. Experimental design and response surface methodology in energy applications: A tutorial review. *Energy Convers. Manag.* **2017**, *151*, 630–640. [[CrossRef](#)]
35. Milano, J.; Ong, H.C.; Masjuki, H.H.; Silitonga, A.S.; Chen, W.-H.; Kusumo, F.; Dharma, S.; Sebayang, A.H. Optimization of biodiesel production by microwave irradiation-assisted transesterification for waste cooking oil-Calophyllum inophyllum oil via response surface methodology. *Energy Convers. Manag.* **2018**, *158*, 400–415. [[CrossRef](#)]
36. Muhammad, G.; Ngicha, A.D.P.; Lv, Y.; Xiong, W.; El-Badry, Y.A.; Asmatulu, E.; Xu, J.; Alam, M.A. Enhanced biodiesel production from wet microalgae biomass optimized via response surface methodology and artificial neural network. *Renew. Energy* **2022**, *184*, 753–764. [[CrossRef](#)]
37. Pinto, D.; Vieira, E.F.; Peixoto, A.F.; Freire, C.; Freitas, V.; Costa, P.; Delerue-Matos, C.; Rodrigues, F. Optimizing the extraction of phenolic antioxidants from chestnut shells by subcritical water extraction using response surface methodology. *Food Chem.* **2021**, *334*, 127521. [[CrossRef](#)]
38. Sharma, P. Prediction-optimization of the effects of Di-Tert butyl peroxide-biodiesel blends on engine performance and emissions using multi-objective response surface methodology. *J. Energy Resour. Technol.* **2022**, *144*, 072301. [[CrossRef](#)]
39. Chen, H.; Wang, M.; Zhao, X. A multi-strategy enhanced sine cosine algorithm for global optimization and constrained practical engineering problems. *Appl. Math. Comput.* **2020**, *369*, 124872. [[CrossRef](#)]
40. Mirjalili, S.; Jangir, P.; Saremi, S. Multi-objective ant lion optimizer: A multi-objective optimization algorithm for solving engineering problems. *Appl. Intell.* **2017**, *46*, 79–95. [[CrossRef](#)]
41. Van Dijk, N.P.; Maute, K.; Langelaar, M.; van Keulen, F. Level-set methods for structural topology optimization: A review. *Struct. Multidiscip. Optim.* **2013**, *48*, 437–472. [[CrossRef](#)]
42. Wang, C.-N.; Yang, F.-C.; Nguyen, V.T.T.; Vo, N.T.M. CFD analysis and optimum design for a centrifugal pump using an effectively artificial intelligent algorithm. *Micromachines* **2022**, *13*, 1208. [[CrossRef](#)] [[PubMed](#)]
43. Yildiz, A.R.; Abderazek, H.; Mirjalili, S. A comparative study of recent non-traditional methods for mechanical design optimization. *Arch. Comput. Methods Eng.* **2020**, *27*, 1031–1048. [[CrossRef](#)]
44. Yildiz, B.S.; Kumar, S.; Pholdee, N.; Bureerat, S.; Sait, S.M.; Yildiz, A.R. A new chaotic Levy flight distribution optimization algorithm for solving constrained engineering problems. *Expert Syst.* **2022**, *39*, e12992. [[CrossRef](#)]

45. Zhang, C.; Sheng, X.; Zhang, S.; Gao, J.; Yuan, T.; Zhang, J.; Li, W. Experiment of influence factors on sawing power consumption for natural rubber mechanical tapping. *Trans. Chin. Soc. Agric. Eng.* **2018**, *34*, 32–37. (In Chinese) [[CrossRef](#)]
46. Zhou, H.; Zhang, S.; Zhai, Y.; Wang, S.; Zhang, C.; Zhang, J.; Li, W. Vision servo control method and tapping experiment of natural rubber tapping robot. *Smart Agric.* **2020**, *2*, 56–64. (In Chinese) [[CrossRef](#)]
47. Liu, X.J.; Li, X.B. The Influence of agricultural production mechanization on grain production capacity and efficiency. *Processes* **2023**, *11*, 487. [[CrossRef](#)]
48. Sayed, H.A.A.; Ding, Q.S.; Abdelhamid, M.A.; Alele, J.O.; Alkhaled, A.Y.; Refai, M. Application of machine learning to study the agricultural mechanization of wheat farms in Egypt. *Agriculture* **2023**, *13*, 70. [[CrossRef](#)]
49. Wang, S.; Hu, Z.; Chen, Y.; Wu, H.; Wang, Y.; Wu, F.; Gu, F. Integration of agricultural machinery and agronomy for mechanised peanut production using the vine for animal feed. *Biosyst. Eng.* **2022**, *219*, 135–152. [[CrossRef](#)]
50. Fan, Y.; Huang, G. Preparation and Analysis of Pueraria lobata Polysaccharides. *ACS Biomater. Sci. Eng.* **2023**, *9*, 2329–2334. [[CrossRef](#)]
51. Li, H.B.; Chen, L.W.; Zhang, Z.Y. A study on the utilization rate and influencing factors of small agricultural machinery: Evidence from 10 hilly and mountainous provinces in China. *Agriculture* **2023**, *13*, 51. [[CrossRef](#)]
52. Li, J.; Shi, H.; Yu, J.; Lei, Y.; Huang, G.; Huang, H. Extraction and properties of Ginkgo biloba leaf polysaccharide and its phosphorylated derivative. *Ind. Crops Prod.* **2022**, *189*, 115822. [[CrossRef](#)]
53. Song, Z.; Xiong, X.; Huang, G. Ultrasound-assisted extraction and characteristics of maize polysaccharides from different sites. *Ultrason. Sonochem.* **2023**, *95*, 106416. [[CrossRef](#)] [[PubMed](#)]
54. Wang, Y.; Xiong, X.; Huang, G. Ultrasound-assisted extraction and analysis of maidenhairtree polysaccharides. *Ultrason. Sonochem.* **2023**, *95*, 106395. [[CrossRef](#)] [[PubMed](#)]
55. Xiong, X.; Yang, W.; Huang, G.; Huang, H. Ultrasonic-assisted extraction, characteristics and activity of Ipomoea batatas polysaccharide. *Ultrason. Sonochem.* **2023**, *96*, 106420. [[CrossRef](#)] [[PubMed](#)]
56. Goncalves, P.D.S.; Silva, M.; Gouvêa, L.; Junior, E. Genetic variability for girth growth and rubber yield in *Hevea brasiliensis*. *Sci. Agric.* **2006**, *63*, 246–254. [[CrossRef](#)]
57. Gouvea, L.R.L.; Silva, G.A.P.; Verardi, C.K.J.Q.; Scaloppi, E.J.; Goncalves, P.D.S. Temporal stability of vigor in rubber tree genotypes in the pre- and post-tapping phases using different methods. *Euphytica* **2012**, *186*, 625–634. [[CrossRef](#)]
58. Sun, Z.; Yang, H.; Zhang, Z.; Liu, J.; Zhang, X. An improved YOLOv5-based tapping trajectory detection method for natural rubber trees. *Agriculture* **2022**, *12*, 1309. [[CrossRef](#)]
59. Wongtanawijit, R.; Khaorapapong, T. Rubber tapping line detection in near-range images via customized YOLO and U-Net branches with parallel aggregation heads convolutional neural network. *Neural Comput. Appl.* **2022**, *34*, 20611–20627. [[CrossRef](#)]
60. Pramchoo, W.; Geater, A.F.; Harris-Adamson, C.; Tangtrakulwanich, B. Ergonomic rubber tapping knife relieves symptoms of carpal tunnel syndrome among rubber tappers. *Int. J. Ind. Ergon.* **2018**, *68*, 65–72. [[CrossRef](#)]

**Disclaimer/Publisher’s Note:** The statements, opinions and data contained in all publications are solely those of the individual author(s) and contributor(s) and not of MDPI and/or the editor(s). MDPI and/or the editor(s) disclaim responsibility for any injury to people or property resulting from any ideas, methods, instructions or products referred to in the content.